

Default Classification of Conical Shaped Charges

Final Summary Task Order Report
Phase 2
DTPH5616D00001/DTPH5617F00019 (TO#0001)

SwRI® Contract Number 01-77494
SwRI® Project Number 22978

Prepared by:

Carl Weiss, M.S.
Keith A. Friedman, Ph.D.
Jimell Erwin, Ph.D.

Prepared for:

U.S. Department of Transportation
Pipeline and Hazardous Materials Safety Administration (PHMSA)
Office of Hazardous Materials Safety Research & Development
1200 New Jersey Avenue, SE
Washington, DC 20590

14 June 2019



SOUTHWEST RESEARCH INSTITUTE®
6220 Culebra Road P.O. Drawer 28510
San Antonio, Texas 78228-0510

SOUTHWEST RESEARCH INSTITUTE®
6220 CULEBRA ROAD • P.O. DRAWER 28510
SAN ANTONIO, TEXAS 78228-0510

Default Classification of Conical Shaped Charges

Final Summary Task Order Report Phase 2

DTPH5616D00001/DTPH5617F00019 {TO#0001}

SwRI® Contract Number 01-77494
SwRI® Project Number 22978

Prepared by:

Carl Weiss, M.S.
Keith A. Friedman, Ph.D.
Jimell Erwin, Ph.D.

Prepared for:

U.S. Department of Transportation
Pipeline and Hazardous Materials Safety Administration (PHMSA)
Office of Hazardous Materials Safety Research & Development
1200 New Jersey Avenue, SE
Washington, DC 20590

Submitted by:

Approved by:

Carl Weiss
Manager
Ballistics & Explosives Engineering Section
Engineering Dynamics Department
Mechanical Engineering Division

Michael G. MacNaughton, Ph.D., P.E.
Vice President
Chemistry & Chemical Engineering Division

TABLE OF CONTENTS

	<u>Page</u>
1. Project Overview	1
2. Phase 2 Testing Overview	2
2.1 Water Capture for Fragment Size Analysis	2
2.2 Blast-Only Experiments	3
2.3 Fragment-Only Experiments	9
2.4 Combined Blast and Fragmentation	14
2.5 Small-Scale Bonfire Testing	16
3. Modeling and Simulation	24
3.1 Fragment Size Analysis	24
3.2 Blast-Only Simulations	27
3.3 Fragment Impact-Only Simulations	31
3.4 Combined Blast and Fragmentation Simulations	32
3.5 Thermal Cook-off Modeling	32
4. Methods for Determining Hazard Classification	34
4.1 Method #2 - Historical Shaped Charge Classification Data (Default)	35
4.2 Method #3 – Hazard Classification through Analytical Modeling	40
4.3 Method #4 – Hazard Classification through Modeling & Simulation (M&S)	41
5. Conclusions on Methodologies	46
6. Recommendations and Further Research	48

LIST OF TABLES

<u>Table No.</u>	<u>Page</u>
Table 1. Fragments for HNS Fill	2
Table 2. Fragments for HMX Fill	2
Table 3. Blast-Only Sympathetic Detonation Results, All Tests	9
Table 4. Fragment-Only Impact Results, All Tests	13
Table 5. Combined Blast and Frag Sympathetic Detonation Results, All Tests	15
Table 6. Summary of Peak Shaped Charge and Flame Temperatures at Flame Extinguishment	23
Table 7. Summary of Package Incident Radiant Heat Flux	23
Table 8. Example Combined N.E.W., M/C Classification by Default Structure	38
Table 9. Visual Comparison of Methods to Develop Default Classification System	48

LIST OF FIGURES

<u>Figure No.</u>	<u>Page</u>
Figure 1. Histogram of Recovered Fragments (HMX and HNS steel-cased charges).....	3
Figure 2. Recovered Fragment Data Analysis (HMX and HNS steel-cased charges).....	3
Figure 3. Geometry of Charges used for Blast-Only Experiments	4
Figure 4. In-Contact Blast-Only Experiment (X-ray Heads in Background)	4
Figure 5. HNS-Filled Shaped Charge Test Results (Steel Cased)	5
Figure 6. HMX-Filled Shaped Charge Test Results (Steel Cased).....	6
Figure 7. Typical Test Setup (Zinc Cased)	7
Figure 8. Recovered Liners and Cases (Zinc).....	7
Figure 9. Zinc-Cased Results – All Tests.....	8
Figure 10. Steel Fragment used for Fragment-Only Experiments	9
Figure 11. Universal Receiver with Rifled Barrel	10
Figure 12. Break-Screen and Zinc Charge Prior to Test (X-ray Head in Background).....	10
Figure 13. Break-Screen and Zinc Charge Prior to Test (X-ray Head in Background).....	11
Figure 14. Point-of-Aim for Fragment-Only Experiments	11
Figure 15. X-ray Images and Velocities for the Zinc-Cased Shaped Charges.....	12
Figure 16. Recovered Cases from Impact Locations #1 and #2.....	13
Figure 17. Low-Order Response at 4,447 fps (Location #3)	13
Figure 18. Typical Test Setup for Combined Blast and Fragmentation.....	14
Figure 19. X-ray Images of Zinc-Cased Charge Response to both Blast and Frag	15
Figure 20. Recovered of the Zinc-Cased Shaped Charge Components	16
Figure 21. Typical Layout for Shaped Charge Packaging (Hexacomb omitted).....	17
Figure 22. Tray Layer (left) and Vapor-Barrier Wrapped Tray inside 4G Box (right).....	18
Figure 23. Typical Setup; Package (top), Pan Fire (left), Wood Crib Fire (right).....	19
Figure 24. Heat Release Rates	20
Figure 25. Package Debris and Surrogate Charges after Test 1.....	20
Figure 26. Bottom Tray Charge Temperatures for Test 1 (top) and Test 2 (bottom)	22
Figure 27. Finite Element Mesh for the Steel-Cased Shaped Charge.....	25
Figure 28. HMX-Filled Steel Case Results.....	25
Figure 29. HNS-Filled Steel Case Results	26
Figure 30. Off-Axis Detonation Results	27
Figure 31. Zinc-Cased Charge (Left) and C-4 Donor (Right).....	28
Figure 32. Zinc-Cased Charge Response to a 22-gram C-4 Donor	29
Figure 33. Steel-Cased Charge Response to a 22-gram C-4 Donor.....	30
Figure 34. Fragment Impact-Only Sympathetic Detonation Simulations.....	31
Figure 35. Combined Blast and Fragmentation (Steel Donor, Zinc Receptor).....	32
Figure 36. Implicit Cook-off Model Results.....	33
Figure 37. Subsequent Detonation Results with an SPH Case	34

Figure 38. Example Vendor Specification Sheet (from DynaEnergetics)	36
Figure 39. Class/Division Assignment as a Function of N.E.W	37
Figure 40. M/C Ratio as a Function of N.E.W. for both 1.1 and 1.4 Shaped Charges	38
Figure 41. Down-Hole Time Rating vs. Temperature (from GEODynamics).....	39
Figure 42. Example Case Geometry with Internal Serrations.....	41
Figure 43. Finite Element Mesh for a Single Tray of Shaped Charges	42
Figure 44. M&S of Intentionally Detonated Shaped Charge Case Fracture and Experimental Data	43
Figure 45. FRC’s Simulations of Thermal Initiation of a Shaped Charge	44
Figure 46. Charge Position in a Simulated Bonfire Test.....	45
Figure 47. Example Package Arrangements for Commercial Shaped Charges	50

1. PROJECT OVERVIEW

Currently, conical shaped charges, especially those developed for use in the oil and gas industry, are classified for transport either by UN Series 6 testing or through analogy that is based on previously characterized designs. Legacy family classification criteria were based simply on the net explosive weight (N.E.W.) of a single device and often referenced testing of larger or similar designs as rational for the appropriate classification of the new item. Other important parameters, such as case thickness and case material, could be varied without the need for additional hazard classification testing. No scientific or engineering rational for such criteria could be found by the Department of Transportation (DoT), the regulatory agency overseeing approval of new EX applications for new energetic designs offered for transport. As such, in 2011, the family classification approval system was halted, and all new energetic device designs were required to undergo formal Series 6 testing.

Shaped charges, specifically oilfield perforation charges, can be designed and fabricated in almost an unlimited number of unique configurations. Additionally, how they are packaged for shipment/storage also contributes to the overall hazards they present in transit. However, due to their method of manufacturing and their end-use, oilfield shaped charges share many common features that may make them appropriate for classification by analogy or other default metrics. Such guidelines, if developed and validated, would streamline the EX approval process, result in lower development costs for industry, and minimize the amount of time it takes to get a new device approved for shipment while promoting safety in transit.

The DoT, through the Pipeline and Hazardous Materials Safety Administration (PHMSA), has funded Southwest Research Institute® (SwRI®) and Friedman Research Corporation (FRC) to conduct fundamental and applied research leading to the development of improved criteria for shipping hazard classification of shaped charges by default. It is intended that guidelines will be backed with experimental data to validate their suitability and limitations. A default classification system, as opposed to analogy-based, was programmatically defined as parameters or metrics, which if adhered to, would result in a correct hazard classification without the need for formal Series 6 testing. Analogy on the other hand, is based purely on previous testing and the assumption that the new device will behave comparably under similar forms of insult.

During the Phase II effort, SwRI and FRC executed the Phase II Research Plan developed during Phase I. The testing included simulated Series 6C testing and controlled blast, fragment, and combined blast and fragment impact experiments to better understand the environments that shaped charges experience during Series 6 testing and the parameters that affect their inherent sensitivity. Detailed computations were done in conjunction to help guide and explain the experiments. A site visit to a commercial shaped charge manufacturer was also conducted to gain more insight to the shaped charge designs, manufacturing process, and the Series 6 testing conducted at the manufacturing facility.

At the completion of the Phase II activity, SwRI and FRC began to draft metrics for classification by default and proposed the additional research necessary to fully develop and verify a comprehensive set of guidelines.

2. PHASE 2 TESTING OVERVIEW

During Phase II, SwRI and FRC expanded on the experimental data generated during Phase 1. The purpose of the testing was to conduct highly controlled and instrumented experiments to better understand the parameters affecting the sensitivity of oilfield perforation shaped charges to sympathetic detonation in the context of Series 6 testing. In Phase 1, SwRI and FRC investigated potential methods of transmission of detonation between charges in their normal shipping configuration and packaging. These methods were tested during Phase II and provided data to validate concurrent modeling and simulation efforts.

Six unique test types were conducted: underwater detonation for fragment capture, blast-only, fragment impact-only, combined blast and fragmentation, simulated bonfire testing, and blast-only package testing. The following sections of this report document the results of this testing.

2.1 Water Capture for Fragment Size Analysis

SwRI detonated steel-cased HMX- and HNS-filled shaped charges at a net explosive weight (N.E.W.) of 23 grams. Additionally, a zinc-cased HMX-filled design of the same charge weight was also detonated. The charges were sealed in 5-gallon buckets and submerged in water to allow for fragment capture after detonation. The 5-gallon bucket allowed the fragments to form before interaction with the water. The fragments were then recovered, weighed, counted, and binned to provide an estimate of the fragments generated during the intentional detonation of the charge (as required in Series 6A/B style testing). The data was used to determine the appropriate fragment sizes for the fragment-only experiments and to validate FRC’s finite element models of the donor charge detonation and subsequent fragmentation. The velocity of these fragments was previously characterized during the Phase 1 testing. A histogram comparing the steel-cased charges is shown in Figure 1. Figure 2 contains additional fragment data for each charge. Tables 1 and 2 contain the binned fragments based on arbitrary weights.

Table 1. Fragments for HNS Fill

(grams)	HNS
<i>Bin</i>	<i>Frequency</i>
0.1	13
0.5	31
1	19
2	8
5	37
10	9
Total	117

Table 2. Fragments for HMX Fill

(grams)	HMX
<i>Bin</i>	<i>Frequency</i>
0.1	77
0.5	79
1	25
2	30
5	31
10	7
Total	249

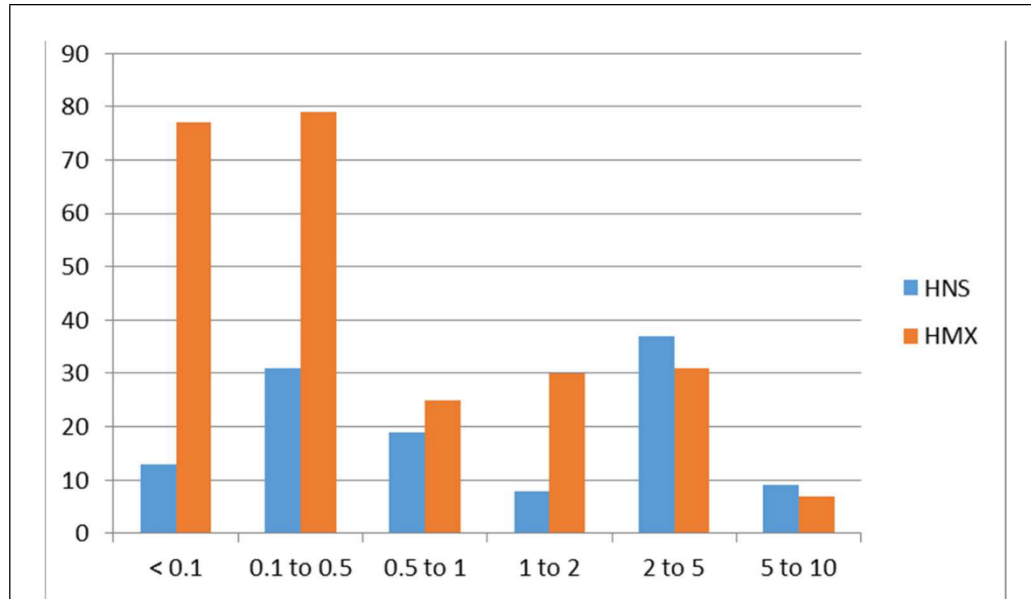


Figure 1. Histogram of Recovered Fragments (HMX and HNS steel-cased charges)

# of fragments	117		# of fragments	249	
% recovered	97.5	%	% recovered	96.1	%
average	1.83	grams	average	0.84	grams
max	8.26	grams	max	7.83	grams
min	0.01	grams	min	0.01	grams
median	0.76	grams	median	0.23	grams
S.D.	1.93	grams	S.D.	1.28	grams
HNS Fill			HMX Fill		

Figure 2. Recovered Fragment Data Analysis (HMX and HNS steel-cased charges)

Data for the zinc-cased charge was omitted due to the extremely small fragments generated by that particular design. It was nearly dust-like and counting and weighing each fragment would have been a significant effort (see Figure 9, Test 11).

2.2 Blast-Only Experiments

During both Phase 1 and Phase 2, SwRI conducted additional blast-only sympathetic detonation experiments to show the potential differences in response between explosive fills (HMX vs. HNS) and case materials (zinc vs. steel). In total, nine (9) valid tests were conducted against three (3) charge configurations. The data was used for model validation and to compare differences in the various shaped-charge parameters on their response.

These sympathetic detonation experiments utilized bare Composition C-4 donor charges at various standoffs until a high-order sympathetic response was noted. Both zinc- and steel-cased HMX-based

charges designs were tested during Phase 2. HNS charges were tested during Phase 1. All receptor charges had a similar N.E.W. of ~23 grams. Repeat experiments were used to confirm the response.

<i>[Not disclosed]</i>	<i>[Not disclosed]</i>
<i>[Not disclosed]</i>	<i>[Not disclosed]</i>

Figure 3. Geometry of Charges used for Blast-Only Experiments

The donor Composition C-4 charges consisted of 22 grams of explosive in a right circular cylinder configuration ($H/D = \sim 1$). They were initiated with an RP-80 or RP-83 exploding bridge-wire detonator located in the top of the charge. The distance between the donor and the receptor was varied depending on the results of previous testing. The charges were placed on foam blocks in a blast containment chamber. The chamber had a viewport on one side to allow for imaging using a 150kV flash x-ray head. A delay generator was used to delay the x-ray exposure at a pre-determined time based on the initiation of the detonator. X-ray film, positioned opposite the charge and x-ray head, was used to capture images of the response of the shaped charge to the blast. The film was protected using thin aluminum, which also served as a witness plate to determine the severity of the charge response. During the majority of testing, two (2) unique x-ray images were taken; one pre-test and one during the detonation event.

[Not disclosed]

Figure 4. In-Contact Blast-Only Experiment (X-ray Heads in Background)

For the HNS-filled charges, a total of two (2) tests were conducted. In both tests, even with the donor explosive in direct contact with the case, no high-order response was noted in the x-ray and in the recovered components. This specific design was very insensitive to initiation from blast alone. Recovered cases were dented with HNS remaining still inside the case. Some residual energetic material was also found on the bottom of the blast chamber after the event. In the x-ray film, copper liner material could be seen being stripped from the shaped charge.

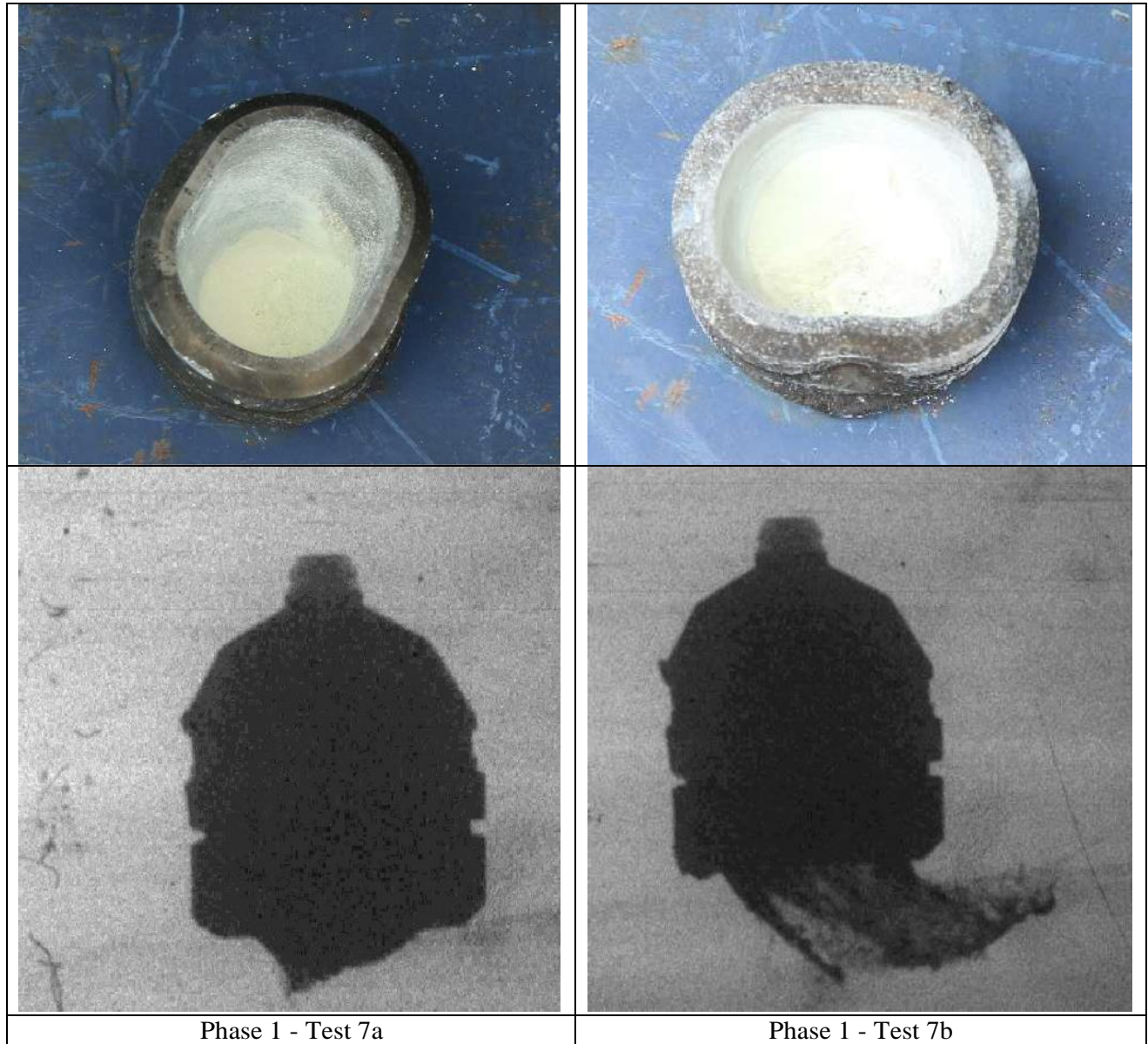


Figure 5. HNS-Filled Shaped Charge Test Results (Steel Cased)

A total of two (2) tests were conducted with the HMX-filled steel cases. In both tests, even with the donor explosive in direct contact with the case, no high-order response was noted in the x-ray and in the recovered components. However, during an in-contact test (no air-gap), the HMX-filled, steel-cased charge underwent a low-order energetic response. This was evident in the resulting x-ray images and in the

recovered case body. It was slightly fractured towards the top of the case, but otherwise suffered minimal damage. These results were slightly more reactive than the HNS-filled charges, which is consistent with the typical sensitivity of the neat explosive formulations.

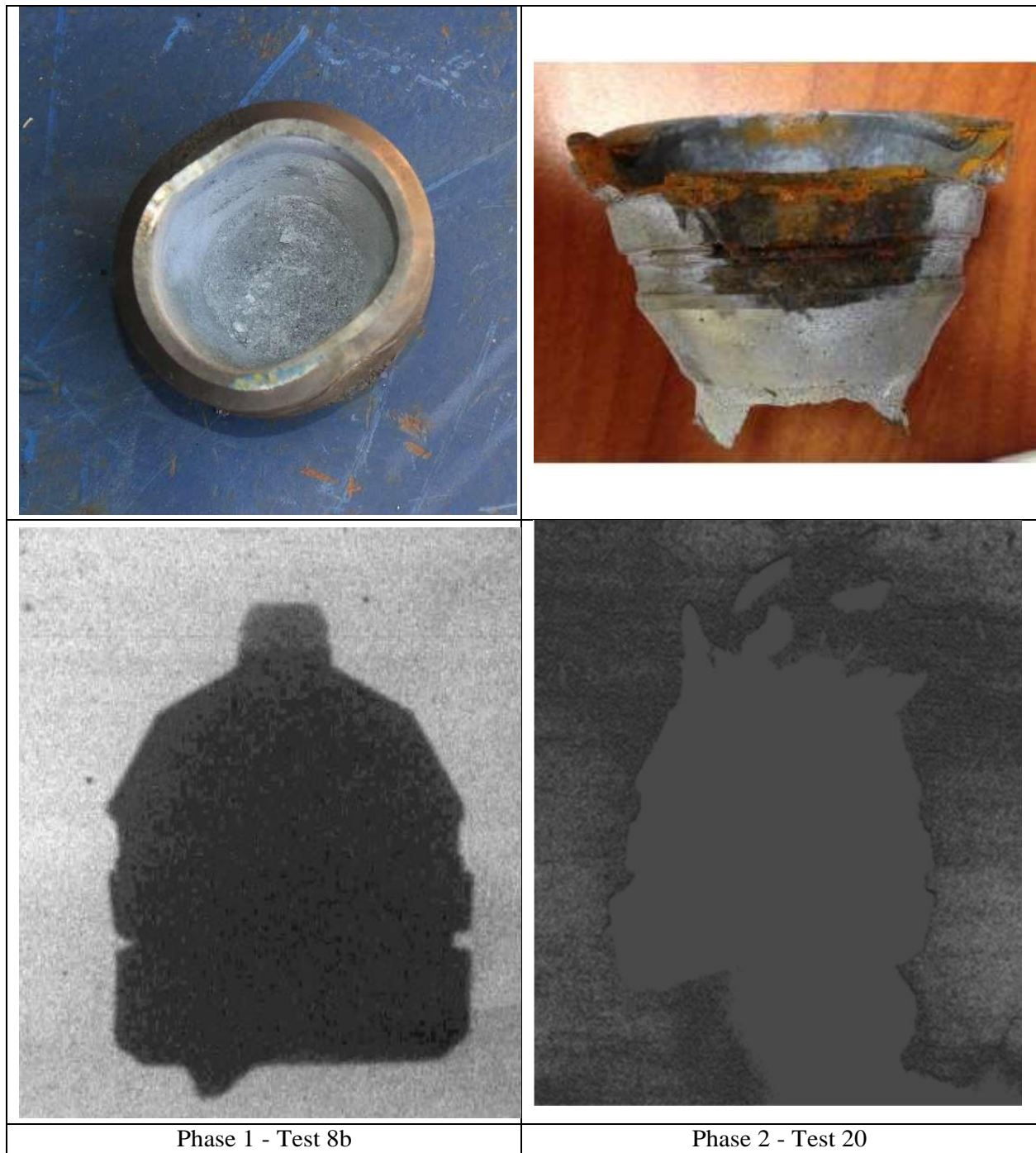


Figure 6. HMX-Filled Shaped Charge Test Results (Steel Cased)

Five (5) unique blast-only sympathetic experiments were conducted with the zinc-cased, HMX-filled charges. Repeat testing was conducted at 0.50-inch air-gap and 0.00-inch air-gap (in-contact) to confirm the results. NO-GO responses were noted during the 0.50 and 1.00 air-gap experiments and high-order

sympathetic response (GO) was noted during both in-contact experiments. Figures 7 and 8, below show the setup for a typical in-contact and air-gaped experiments, along with compiled results.

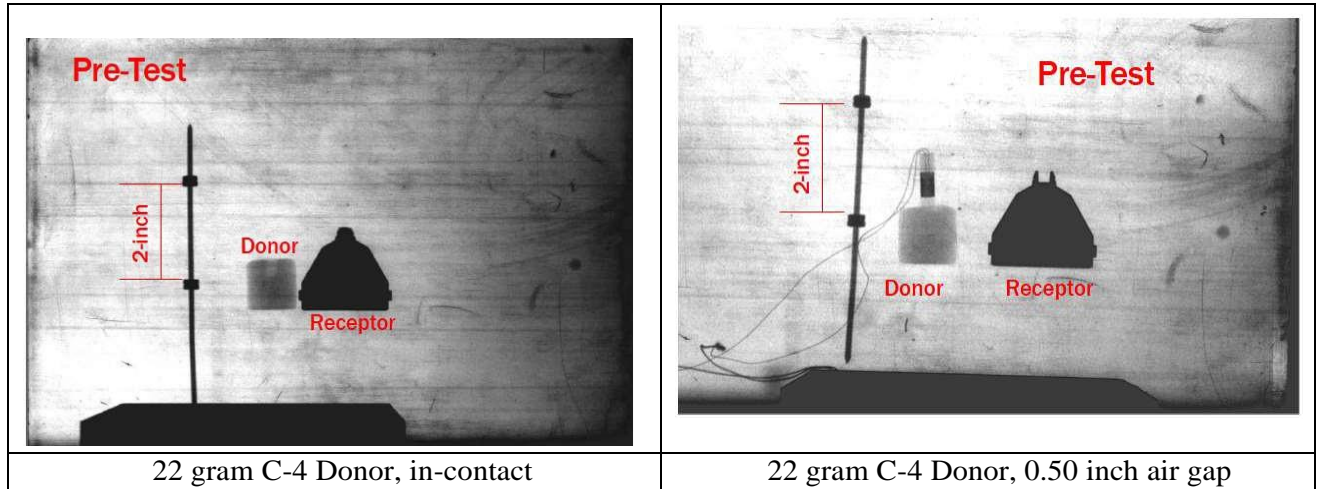


Figure 7. Typical Test Setup (Zinc Cased)

[Not disclosed]

Figure 8. Recovered Liners and Cases (Zinc)

	<i>[Not disclosed]</i>	<i>[Not disclosed]</i>

Figure 9. Zinc-Cased Results – All Tests

As expected, the thinner, lighter, zinc-cased charges responded more severely to blast-only stimuli compared to both the HNS- and HMX-filled, steel-cased shaped charges. N.E.W. was similar for all charge configurations regardless of case material. This indicates that N.E.W. alone is not the only important factor

when assessing the inherent sensitivity of shaped charges to sympathetic initiation. Table 3 contains the results of all testing for visualization purposes.

Table 3. Blast-Only Sympathetic Detonation Results, All Tests

Zinc Cased Charge					Steel Cased Charge				
Test #	Phase #	Explosive Fill	Air Gap (inch)	GO/NO GO	Test #	Phase #	Explosive Fill	Air Gap (inch)	GO/NO GO
12	2	HMX	1.00	No Go	7a	1	HNS	0.10	No Go
13	2	HMX	0.50	No Go	7b	1	HNS	0.00	No Go
19	2	HMX	0.50	No Go	8b	1	HMX	0.10	No Go
11	2	HMX	0.00	Go	20	2	HMX	0.00	Low Order
18	2	HMX	0.00	Go					

2.3 Fragment-Only Experiments

During this effort, SwRI conducted 13 unique fragment-only impact experiments against two (2) 1.4D shaped charge designs. Both shaped charges had a similar explosive fill (HMX-based) and N.E.W. (23 grams). However, their case materials differed (zinc and steel) and there were significant differences in the case and explosive cross-sections. The purpose of the testing was to determine the velocity threshold at which a high-order response was noted in the receptor and to document differences in their responses.

The steel fragments were cylindrical in shape with a length of 0.356 inches and a diameter of 0.343 inches. Their nominal weight was 4.13 grams, which is near the upper end of the expected fragment mass based on the water capture tests (Section 2.1). They were machined from 4340 steel and had a nominal hardness of Rc-30. There was a small skirt machined into the base of the cylinder to allow it to be spin-stabilized when fired from a 0.375-caliber rifle barrel chambered in .375 H&H Magnum. The propellant load in the cartridge case was varied to achieve the desired impact velocity.

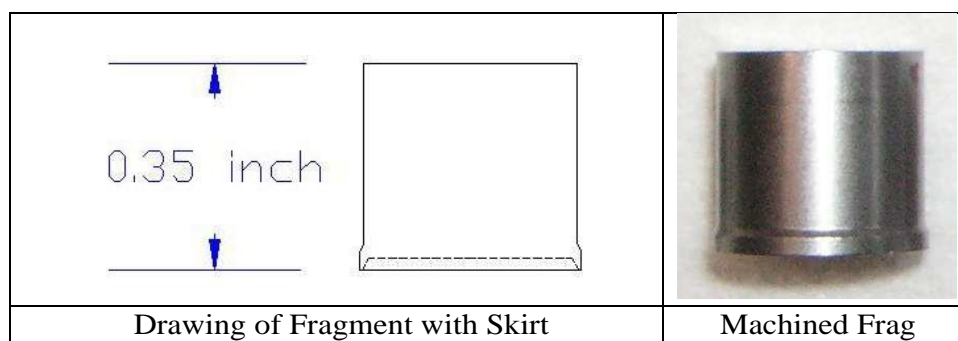


Figure 10. Steel Fragment used for Fragment-Only Experiments

The fragments were fired using a rifled barrel mounted in a universal style receiver. This allowed for a precise point-of-aim and remote firing of the gun (for safety reasons) via pneumatic actuator and lanyard. The gun was mounted outside a blast chamber and aimed through a small hole in the side of the chamber through which the projectile could pass. This allowed the blast and fragments from the shaped charge to be contained to protect the nearby x-ray equipment and personnel. This was the same chamber utilized previously in the blast-only experiments.

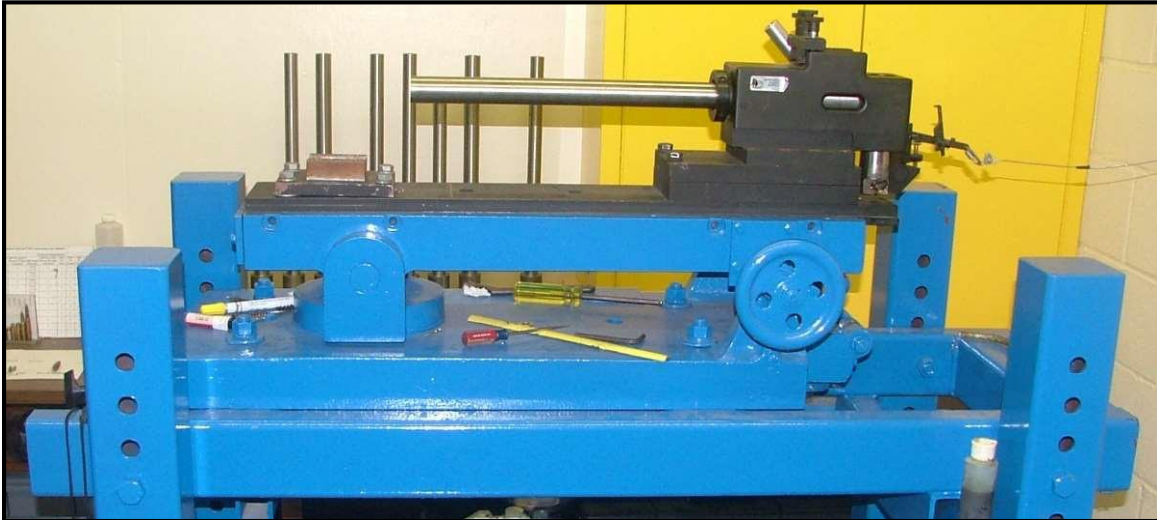


Figure 11. Universal Receiver with Rifled Barrel

Muzzle velocity was monitored using a MagnetoSpeed v3, barrel-mounted chronograph. Break-screens were used to provide a redundant velocity measurement just prior to impact and to trigger the flash x-ray. A single 150 kV flash x-ray system was used to image the charge just after projectile impact based on a specified delay (~100 us) from the last break-screen.

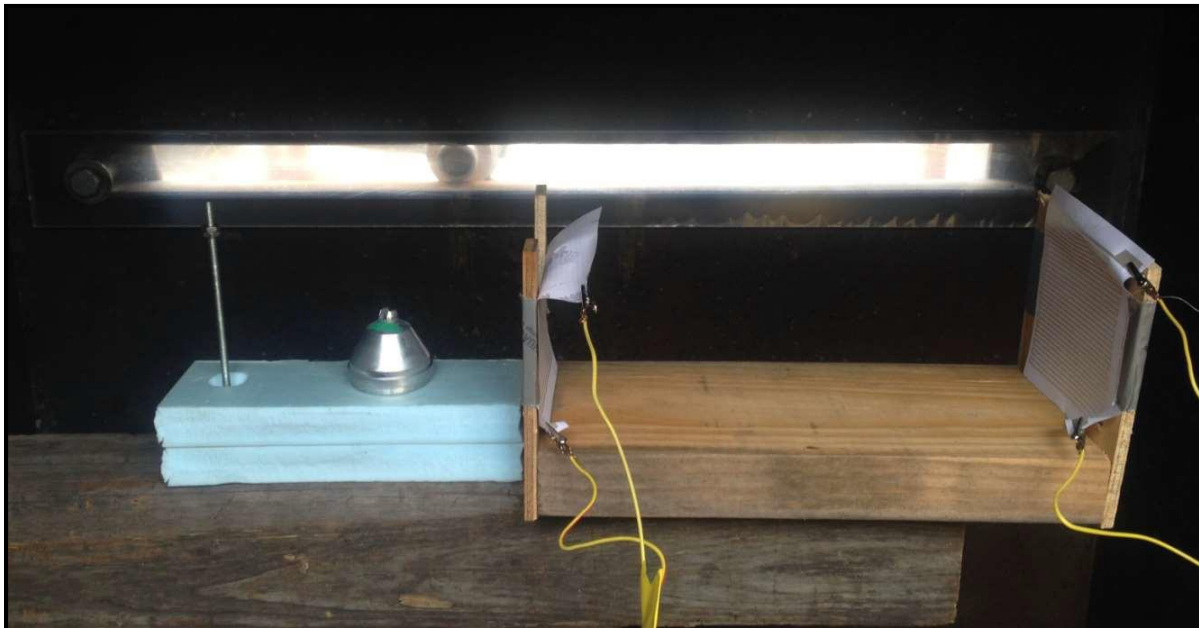


Figure 12. Break-Screen and Zinc Charge Prior to Test (X-ray Head in Background)

The test charges were positioned on the shot-line in front of a small viewport in the side of the blast chamber. The viewport allowed the 150 kV flash x-ray to be aimed into the chamber and image the shaped charges during impact. Film cassettes, opposite the charge and x-ray head were used to protect the film and capture images of the charge response. The front of the film cassette utilized a simple aluminum witness plate to assess the severity of response of the receptor. Any fragmentation, indicative of a high-order response, would result in cratering of the witness plate. For tests with the steel-cased charges, a heavy steel block

was used beneath the charge to determine if a significant shaped charge jet had been formed (another sign of high-order response). Due to concerns about fragmentation penetrating the film cassette, no x-rays were taken during these tests.

[Not disclosed]

Figure 13. Break-Screen and Zinc Charge Prior to Test (X-ray Head in Background)

For the zinc-cased charges, all shots were aimed at the lower portion of the shaped charge cone, where the case material was the thickest and the explosive was the thinnest. This was done with the hopes of providing the best possible chance of no response or low-order response (thickest case buffer and lowest run to detonation distance). For the steel-cased charges, the point-of-aim was varied from test to test due to the insensitivity of the charges as noted during testing. Three (3) unique points-of-aim were utilized (Figure 14) for the steel-cased charges.

<i>[Not disclosed]</i>	<i>[Not disclosed]</i>
Point-of-Aim for Zinc-Cased Charges	Point-of-Aim for Steel-Cased Charges

Figure 14. Point-of-Aim for Fragment-Only Experiments

For the zinc charges, impact velocities were varied from nearly 4,500 fps down to 2,900 fps. With the exception of an anomaly at approximately 4,050 fps, all other tests resulted in the high-order initiation of the donor charge. X-ray images and post-test inspections of the blast chamber were used to confirm the response. A total of six (6) tests were conducted against this shaped-charge design before testing was halted. These results indicate that even at velocities below 3,000 fps, a steel fragment alone was sufficient to shock initiate the main explosive billet.

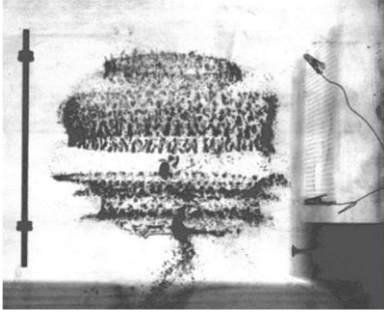
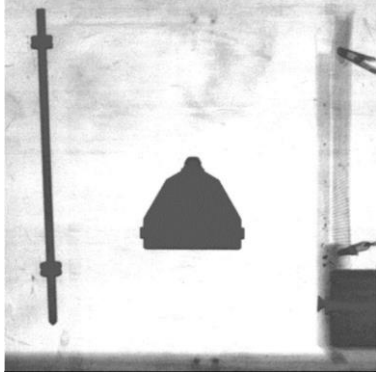
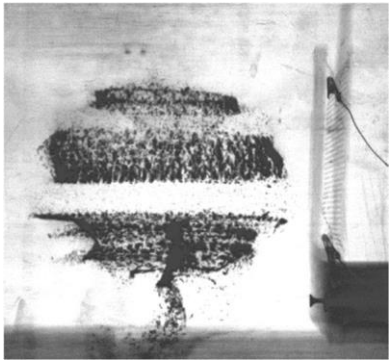
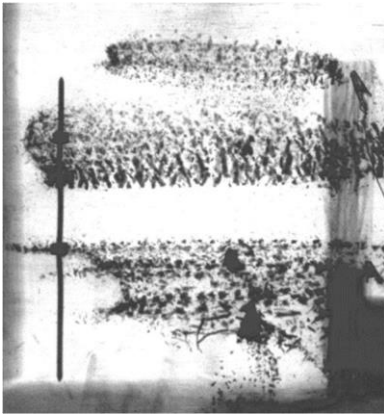
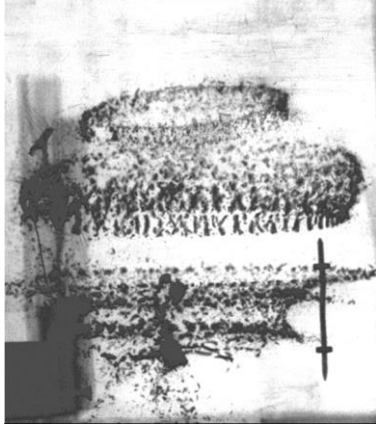
		
Test 01 – 4,456 fps	Test 02 – 4,047 fps (Pre-Test X-ray Only)	Test 03 – 4,074 fps
		
Test 04 – 3,599 fps	Test 05 – 3,301 fps	Test 06 – 2,980 fps (Poor X-ray Contrast)

Figure 15. X-ray Images and Velocities for the Zinc-Cased Shaped Charges

Table 4 outlines the results from the testing of the steel-cased shaped charges. Even at impact velocities as high as 4,305 fps, no response was noted in the recovered steel-shaped charge bodies. During testing at Location #1, three (3) repeat tests were conducted at impact velocities up to 3,878 fps. Partial and complete perforations of the case wall were noted but no high-order response was noted. Similar results were seen at Location #2 at velocities up to 4,039 fps. Post-test recovered steel cases from both impact locations are shown Figure 16.

Only one (1) low-order response was seen during testing. It occurred at an impact velocity of 4,447 fps with the shot aimed at Location #3. The steel case did not fragment, but was found significantly deformed inside the blast chamber (Figure 17). The witness block under the charge showed no evidence of a shaped charge jet being formed.

Table 4. Fragment-Only Impact Results, All Tests

Zinc Cased Charge			Steel Cased Charge			
Test #	Velocity (fps)	GO/NO GO	Test #	Location #	Velocity (fps)	GO/NO GO
6	2,980	Go	1	1	2,850	No Go
5	3,301	Go	2	1	2,785	No Go
4	3,599	Go	3	1	3,878	No Go
2	4,047	No Go	4	2	4,039	No Go
3	4,074	Go	5	2	3,955	No Go
1	4,456	Go	6	3	4,447	Low Order
			7	3	4,305	No Go

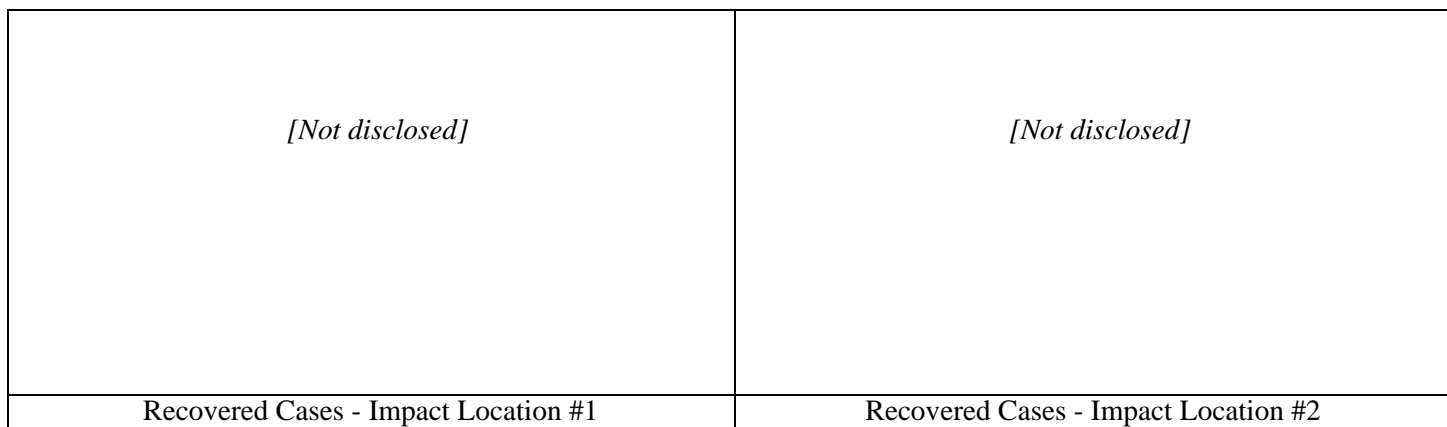


Figure 16. Recovered Cases from Impact Locations #1 and #2



Figure 17. Low-Order Response at 4,447 fps (Location #3)

This test series highlights the differences between two (2) shaped charge designs with the same energetic formulation and quantity. Although both had a N.E.W. of 23 grams of an HMX-based explosive, they responded very differently to single fragment impacts. Although there were variations in the exact charge case geometry, these results indicate that a N.E.W. metric alone is not sufficient to describe the inherent sensitivity of a charge to external stimuli. It should be noted that all velocities used during this testing were well in excess of the velocities characterized for these charges during the Phase 1 effort (1,640 – 2,600 fps). Additionally, steel fragments would not be generated during a Series 6 test with zinc-cased charges.

2.4 Combined Blast and Fragmentation

A series of experiments were then conducted using the zinc-cased receptors and either a steel-cased or zinc-cased donor. The purpose of these experiments was to determine if the charges could initiate a sympathetic response due to combined blast and fragmentation. Also, a paired zinc-cased experiment was conducted to determine if in-contact 1.4D shaped charges, without their interior packaging dividers, would respond sympathetically.

The charges were placed in a blast chamber and the donor charge was command detonated using an RP-87 EBW-style detonator. The test charges were positioned on the shot-line in front of a small viewport in the side of the blast chamber. This viewport allowed the 150 kV flash x-rays to be aimed into the chamber and image the shaped charges during the event. Film cassettes, opposite the charge and x-ray head, were used to protect the film and capture images of the charge response. The front of the film cassette utilized a simple aluminum witness plate to assess the severity of response of the shaped charge. Any fragmentation, indicative of a high-order response, would be result in cratering of the witness plate.

[Not disclosed]

Figure 18. Typical Test Setup for Combined Blast and Fragmentation

During testing, the zinc-cased receptor underwent no response to a zinc-cased donor at an in-contact and 1.00-inch air-gap arrangement. This indicates that, for this particular design, the interior dividers used in the packaging would not be required to prevent detonative transmission between charges (Series 6A/B). It

was also observed that a steel donor, even with its heavier steel fragments, was not able to initiate the zinc-cased receptor at a 1.00-inch spacing. This was slightly unexpected given the results of the Fragment-Only testing. Table 5 below contains a summary of the combined blast and fragmentation experiments. Figure 19 shows the response of a zinc-cased charge to both a zinc- and steel-cased donor. Figure 20 shows typical recovered cases from these experiments.

Table 5. Combined Blast and Frag Sympathetic Detonation Results, All Tests

Zinc-Cased Charge Donor			
Test #	Donor	Air Gap (inch)	GO/NO GO
14	Zinc	0.00	No Go
15	Zinc	1.00	No Go
16	Steel	1.00	No Go

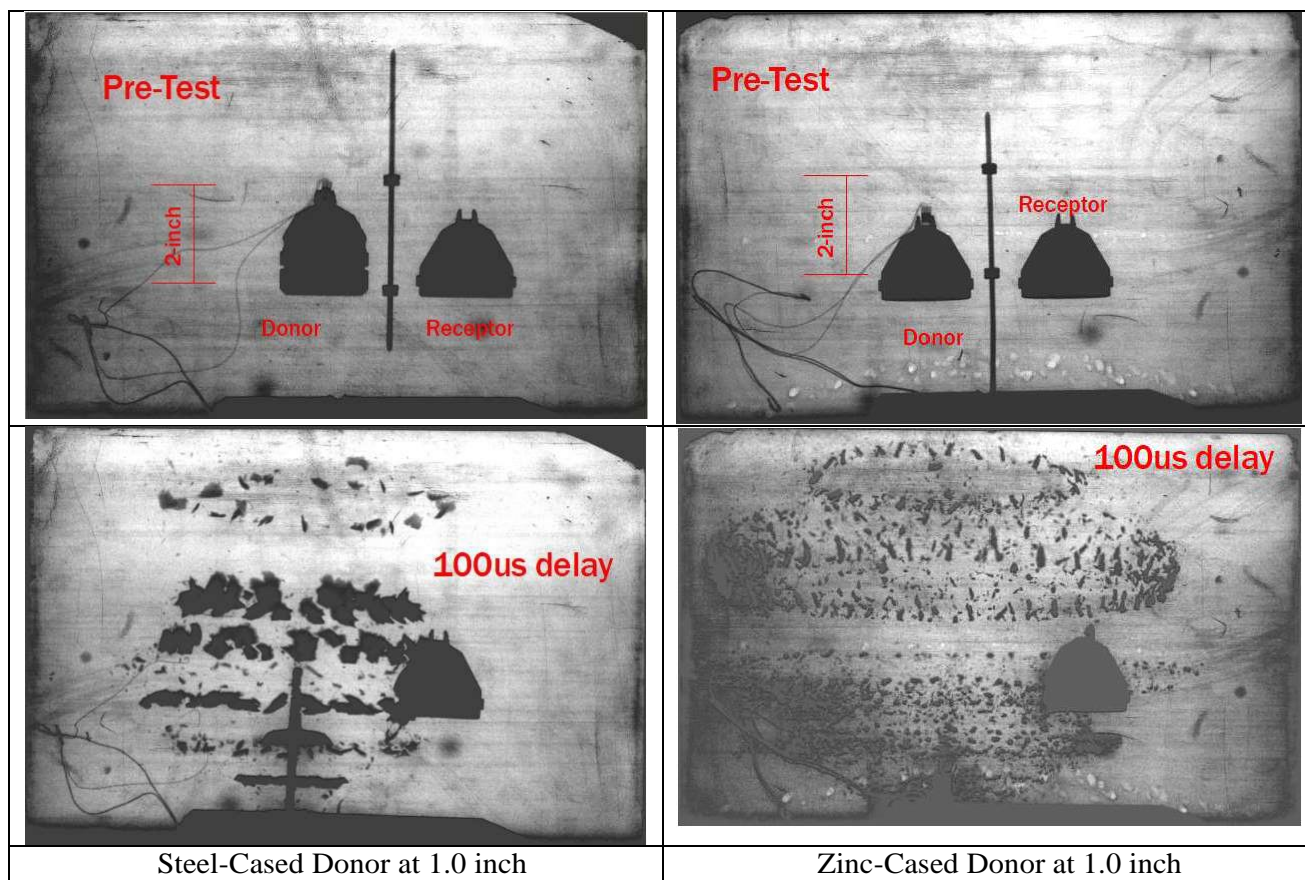


Figure 19. X-ray Images of Zinc-Cased Charge Response to both Blast and Frag

<i>[Not disclosed]</i>	<i>[Not disclosed]</i>
Steel-Cased Donor at 1.0 inch	Zinc-Cased Donor at 1.0 inch

Figure 20. Recovered of the Zinc-Cased Shaped Charge Components

2.5 Small-Scale Bonfire Testing

FRC designed and directed small-scale bonfire testing, conducted at SwRI’s Fire Technologies facility, to generate thermal data during the bonfires and better understand the thermal environment generated during Series 6C testing. Four (4) bonfire tests, using two (2) different fuel sources (Isopropyl Alcohol (IPA) and a wood crib), were conducted to evaluate the thermal loads applied to an exemplar package of surrogate shaped charges. Packaging provided by Hunting Titan, a Texas-based shaped charge manufacturer, was used in this test series. A diagram of typical packaging is provided in Figure 21. The packaging consisted of an exterior UN-4G/Y29.5/S/18 fiberboard box filled with 50 surrogate shaped charges. This is a UN-certified, double-walled box (4G) with a maximum capacity of 29.5 kg (Y29.5) for solid materials (S). The box was manufactured in 2018. Each package contained two (2) trays with a capacity for holding 25 shaped charges (Figure 22). Each tray was wrapped with a foil vapor barrier bag.

[Not disclosed]

Figure 21. Typical Layout for Shaped Charge Packaging (Hexacomb omitted)

Steel cylinders were used as inert surrogate shaped charges. Five (5) surrogate shaped charges in each tray were outfitted with three (3) thermocouples each. The instrumented shaped charges were located in each corner and in the center position in each tray. The thermocouples were positioned along the centerline at 120-degree separation. Plate thermometers were used in Test 1 (IPA Pan Fire) and in each of the wood crib fire tests. They were not used during Test 2 in order to quantify their effect on the heat transfer into the packaging. The plate thermometers were positioned at the center of each face of the package. A gas thermocouple was positioned at the bottom of the package during Tests 2 – 4. All tests were conducted inside a calorimeter to measure the Heat Release Rate (HRR).



Figure 22. Tray Layer (left) and Vapor-Barrier Wrapped Tray inside 4G Box (right)

Two (2) tests were conducted using IPA as the fuel in a pan/pool fire scenario. The fuel pan was 27 inches long x 27 inches wide x 10 inches tall. Fuel was added during each test to maintain the flame. The top of the pool was approximately 1 foot below the bottom of the package.

Two (2) burns were conducted using a 3-A wood crib, which consists of 18 layers of eight (8) wood members each, with dimensions of 2 inches long x 2 inches wide x 29 inches tall. The overall dimensions of the wood-crib were 29 inches long x 29 inches wide x 36 inches tall. The moisture content of each wood crib was measured as 8.7% and 9.2%. Each of the wood cribs was ignited with 3.5 L of IPA, which burned off in approximately four (4) minutes. The top of the crib was initially approximately 1 foot below the bottom of the package in Test 3 (Wood Crib Fire) and directly adjacent to the bottom of the package in crib fire Test 4 (Wood Crib Fire).

A view of the typical test setup is provided in Figure 23.



Figure 23. Typical Setup; Package (top), Pan Fire (left), Wood Crib Fire (right)

The HRR during each test is shown in Figure 24. Both wood crib fires produced maximum HRRs of twice that of the pool fire. During the IPA pan fire, HRR was consistent throughout the test at approximately 590 kW. After peaking, the HRR of the wood crib fire plateaued at around 900-1000 kW before rising rapidly to 1100 kW right before collapse. Each of the wood cribs fires collapsed at approximately 17 minutes. The two IPA tests were conducted for 20 and 29 minutes as reflected in their HRR curves.

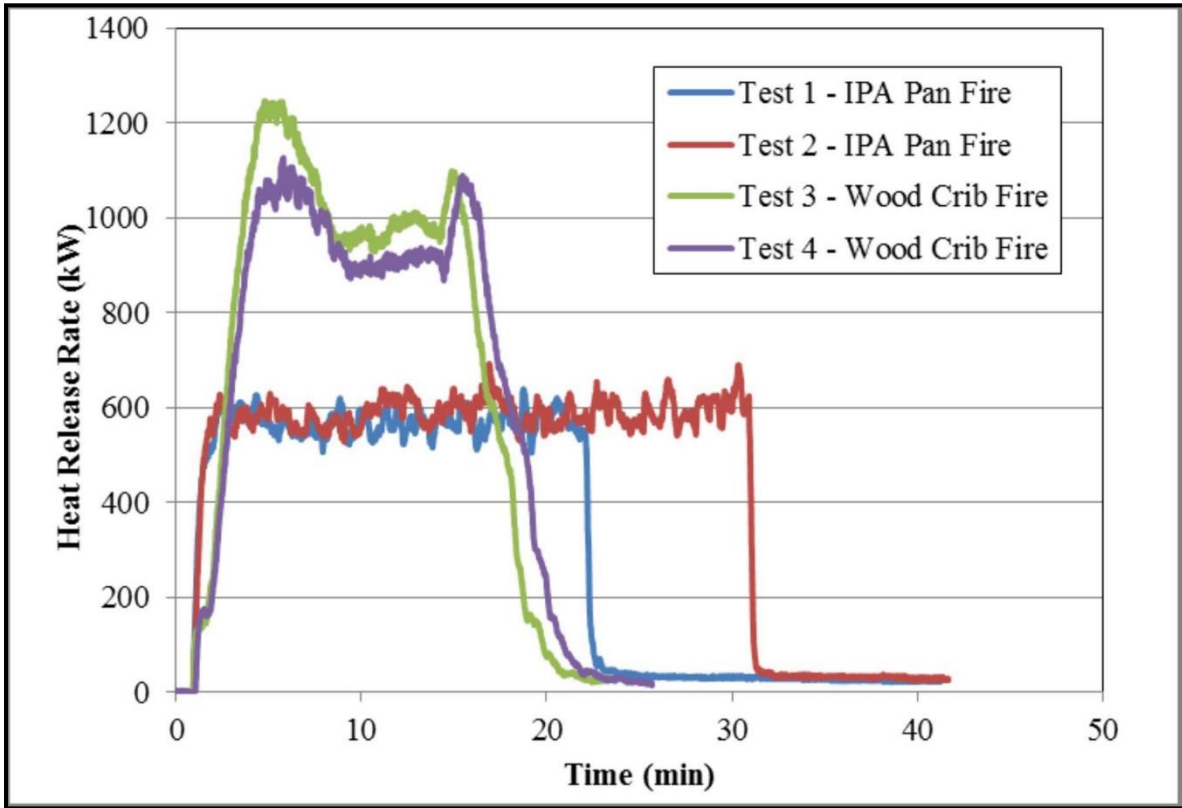


Figure 24. Heat Release Rates

The exterior packaging was mostly consumed in the fire as shown in Figure 25. Remnants of the foil vapor bag and the internal trays were visible after the fire was extinguished. The heat from the bonfire caused the steel support mesh to deform. Vertical mesh deformation varied between 1 and 12 inches. The surrogate shaped charges were typically found in a pile representing their initial positions, but with those located on the exterior having fallen or tilted off-axis.



Figure 25. Package Debris and Surrogate Charges after Test 1

The plate thermometer had a significant effect on the temperature of the central surrogate shaped charge during Test 1 (IPA pan fire) as shown in Figure 26. During Test 2 (IPA pan fire), the central shaped charge in the bottom tray recorded the highest temperature (710°C at 20 minutes; 804°C at 21 minutes) of any shaped charge. (Recall that Test 1 was conducted for 20 minutes and Test 2 was conducted for 29 minutes.) In Test 1, the central shaped charge reached 271°C at 20 minutes and then continued heating due to the heat transfer from neighboring material after the fire was extinguished. The plate thermometer appeared to have a minor effect on the shaped charges located in the corners. Similar results were observed for the top tray.

Shaped charge temperatures ranged from 220 – 800°C depending on the fuel type, presence of plate thermometers, and location of the shaped charge (see Table 26 for details). Greater maximum temperatures were achieved in the IPA pan fire scenario than in the wood crib fire scenario by about 160°C. The maximum flame temperatures measured in the IPA pan fires were greater than those measured in the wood fire by about 50°C. The wood crib fires had peak temperatures reach 1000°C upon collapse, but otherwise had temperatures on the order of 650 – 700°C.

The primary method of heat transfer was via radiation. The incident radiant heat flux was measured in Tests 1, 3, and 4. The bottom and sides of the package experienced a greater incident heat flux from the pan fire than from the wood crib fire. The incident heat flux to the top of the package was similar for all tests (Table 7).

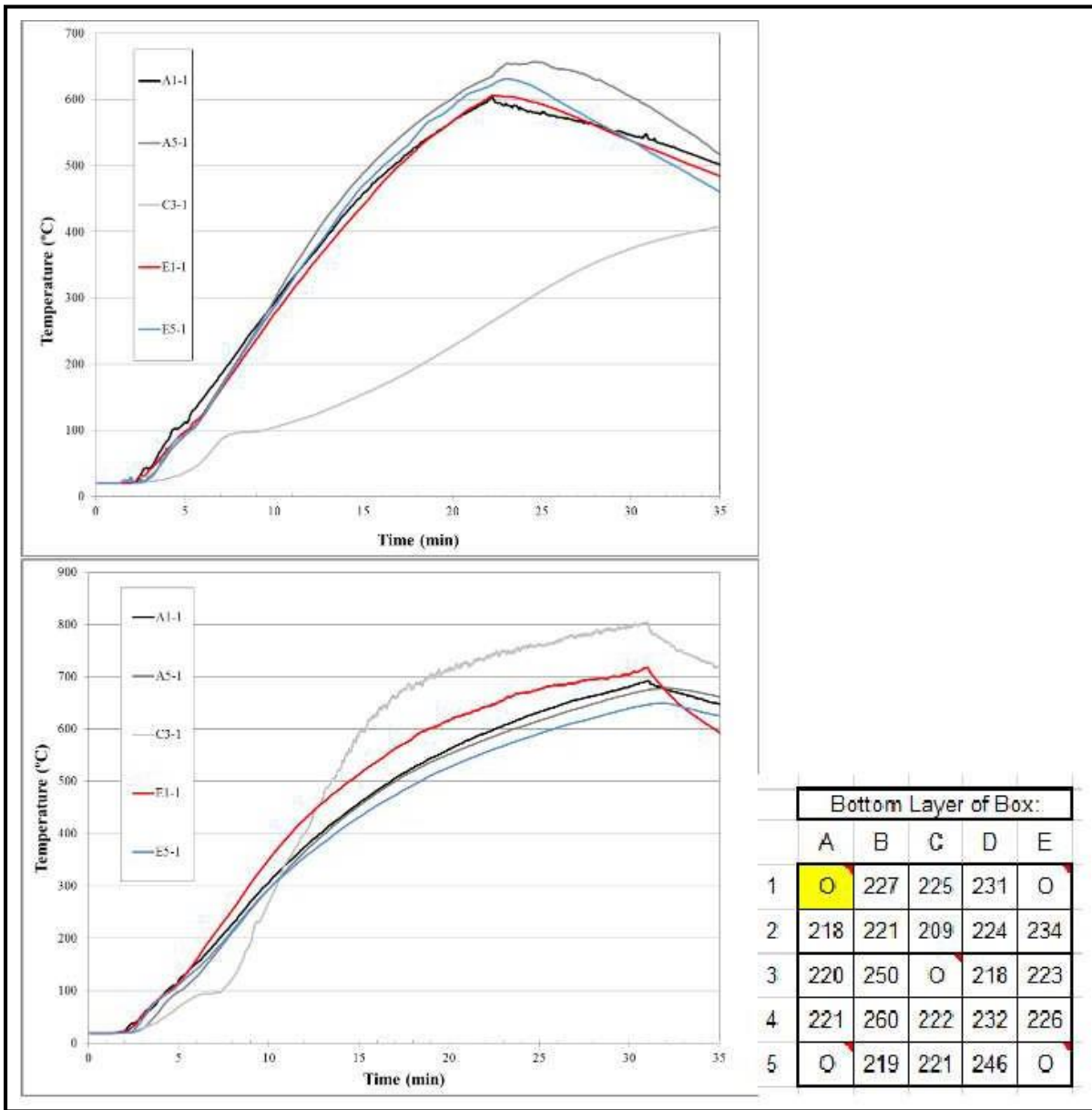


Figure 26. Bottom Tray Charge Temperatures for Test 1 (top) and Test 2 (bottom) Shaped Charge Location Diagram (bottomright)

Table 6. Summary of Peak Shaped Charge and Flame Temperatures at Flame Extinguishment

Test	Top Tray (° C)		Bottom Tray (° C)		Package Perimeter (° C)	
	Min	Max	Min	Max	Min	Max
Test 1 (IPA pan fire)	300	727	271	664	580	785
Test 2 (IPA pan fire)	605	743	646	801	n/a*	850
Test 3 (Wood crib)	220	559	378	507	627	726
Test 4 (Wood crib)	254	536	384	535	629	705

*flame temperature was only measured in one location

Table 7. Summary of Package Incident Radiant Heat Flux

Test	Maximum Heat Flux (kW/m ²)		
	Bottom	Sides	Top
Test 1 (IPA pan fire)	67.2	72.6	44.0
Test 2 (IPA pan fire)	n/a*	n/a*	n/a*
Test 3 (Wood crib)	56.7	57.1	47.7
Test 4 (Wood crib)	n/a*	52.3	42.7

*not measured

The differences in heat output by fuel source are likely to affect the performance of shaped charge during a bonfire test. The fuel used in the IPA pan fire has a relatively low HRR compared to other commonly available fuels. The IPA pan fire produced 590 kW. Assuming the same pan fire conditions, Diesel would have produced 750 kW, Gasoline would have produced 907 kW, Heptane would have produced 1213 kW, and Butane would have produced 1467 kW.

Due to the nature of a wood crib or pallet stack, these types of fires have a limited duration, an irregular HRR, and less predictable thermal output due to variations in moisture content, wood type, and geometry. The benefit of pan fires is that they are more predictable and controllable.

The layout of the surface onto which the package is placed has an effect on the temperatures obtained by the shaped charges. It was obvious that the bottom plate thermometer in the tests caused the central shaped charges to heat much more slowly than those on the perimeter.

The Series 6 test requirements define peak flame temperatures that need to be achieved during the test. There is no HRR requirement. Based on this test and data from the literature, there is a wide range of HRR and flame temperatures that can be produced from different fuels and application methods. In the wood crib fires, the flame temperature near the package only exceeded 800°C at the point in which the crib collapsed. In Test 2 (IPA pan fire) the flame temperature at the base of the package was maintained at a relatively steady 825°C. The location of the peak flame temperature in a wood fueled fire will change as the wood is consumed and may not correspond to the location of the test package.

Of additional consideration is that typical Series 6C bonfire testing uses a “floating” steel mesh to support the packages above the wood crib. As the crib burns down, the steel mesh also moves downward with the fuel source, keeping the charges in closer proximity to the flames. It is recommended that these experiments be repeated during future research to better understand this physical response.

3. MODELING AND SIMULATION

To supplement the Phase II experiments, both SwRI and FRC conducted detailed simulations of the small-scale experiments. The purpose was to guide the experiments, achieve impact conditions not possible during firings, and better understand the modes of sympathetic response. To capture the interior shaped charge geometry, SwRI used CT inspection to digitize the geometry. This allowed for accurate modeling of the exact charges used during testing. The following sections of the report detail the results of the computations and comparison to the experimental data.

3.1 Fragment Size Analysis

FRC conducted intentional detonation simulations of the steel-cased shaped charge with both HNS- and HXM-based explosive fills. The purpose of these simulations was to estimate the velocity and fragment size distributions of the resulting case fragments. This is important for blast and fragment induced sympathetic response in Series 6A/B-type testing. The captured CT geometries were used to generate detailed finite element models of the case, liner, and explosive fill. Where possible, symmetry was exploited to minimize run times and computational domains. The model results were then queried and compared to the experimental data from the water capture experiments in Phase II and the fragment velocity x-ray images captured during Phase I. Output included histograms of the number, size, and velocity/trajectory of the resulting case fragments.

[Not disclosed]

Figure 27. Finite Element Mesh for the Steel-Cased Shaped Charge

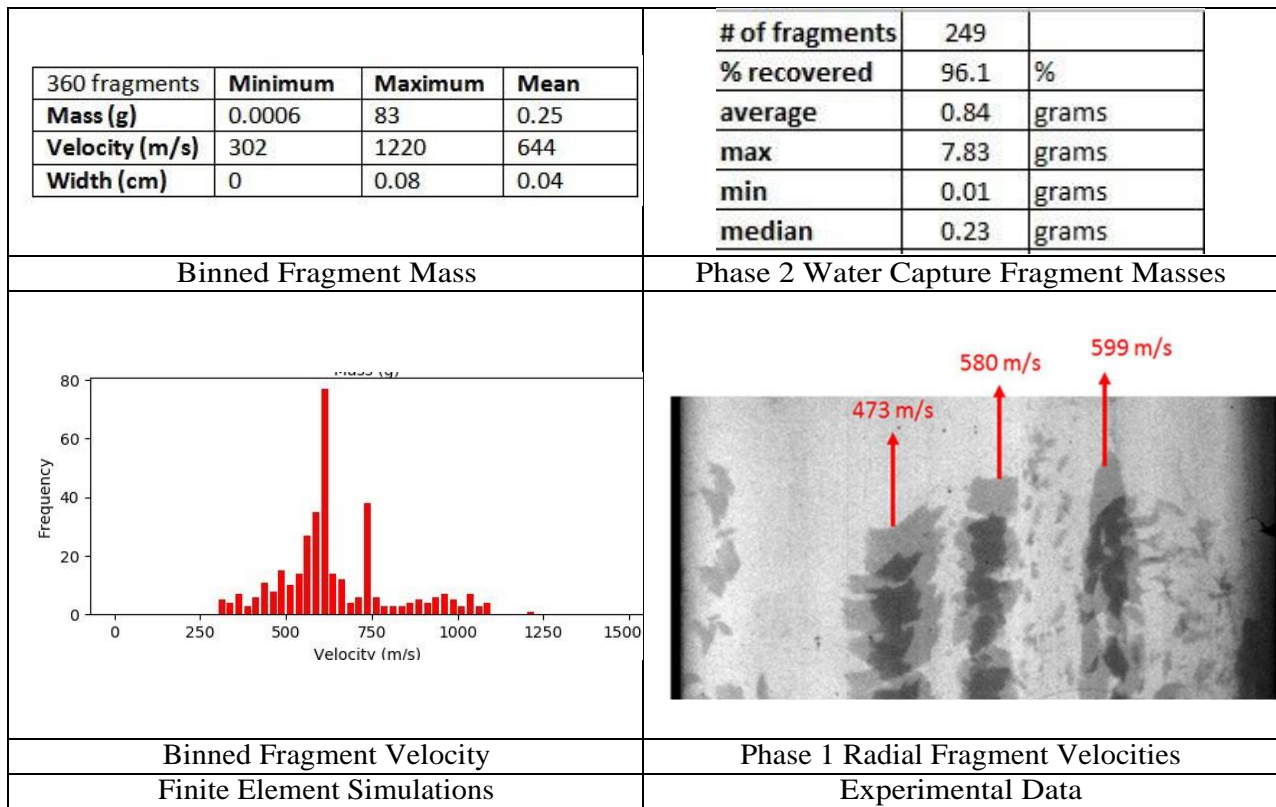


Figure 28. HMX-Filled Steel Case Results

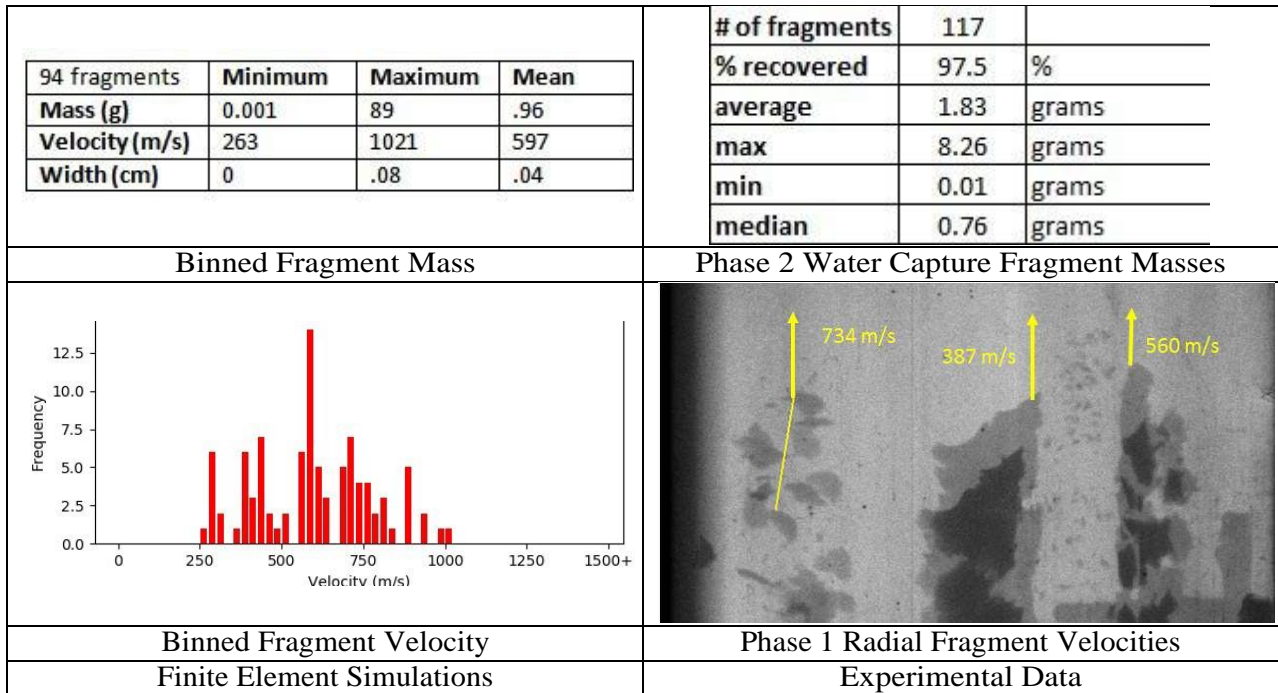


Figure 29. HNS-Filled Steel Case Results

The figures above provide a brief comparison of the test data from the water capture test data vs. the finite element results. There is general agreement between the total number of expected fragments, the median size, and the performance of HMX vs. HNS in terms of the fragments generated. However, there is some discrepancy between the maximum fragment size and the velocity of the resulting fragment field. The finite element analysis indicates much higher velocity magnitudes than the radial velocities determined experimentally during Phase I. The output highlights the usefulness and limitations of a simulation-only approach.

In a second study, the charge was detonated based on the expected location of thermal runaway from a simulated heating event rather than from the traditional top-dead-center location. The purpose of this simulation was to understand the difference in the resulting fragment field in terms of expected numbers, representative masses, and expected velocity ranges. The offset detonation charge was initiated near the base of the liner where temperatures were highest. Figure 30 provides a side-by-side comparison in the results.

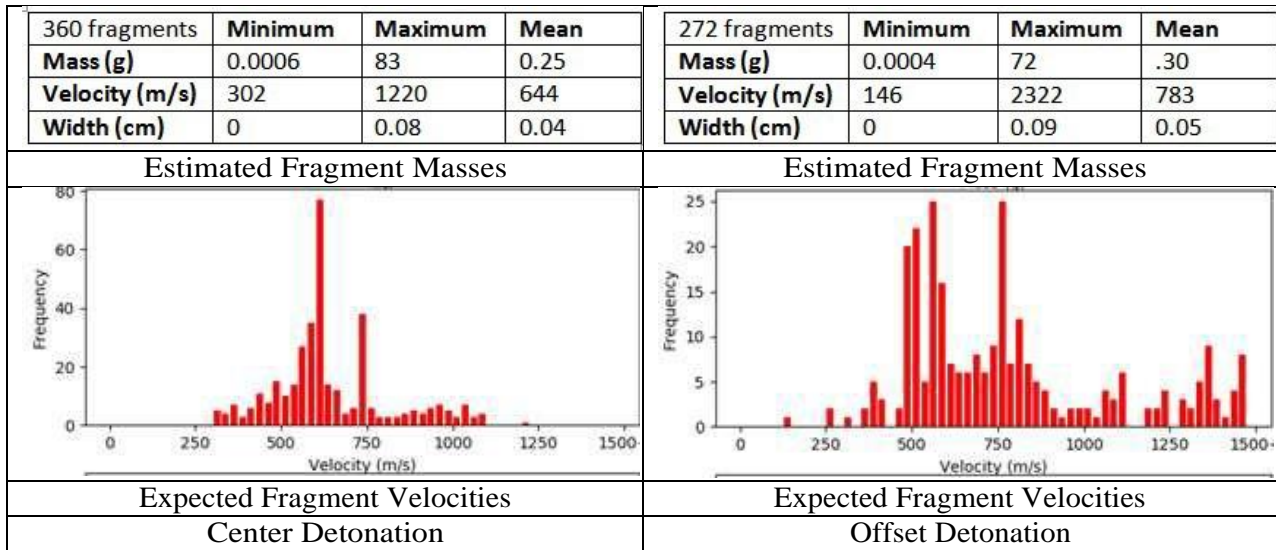


Figure 30. Off-Axis Detonation Results

A larger range of expected velocities was noted in the off-axis detonation case in addition to a much higher magnitude. Additionally, with a lower number of estimated fragments, the average mass of the fragments went up slightly. Larger, faster moving fragments have a higher potential to initiate neighboring charges. This set of simulations would be important for estimating the response of neighboring charges in a Series 6C test where a donor charge underwent a high-order response due to thermal insult.

3.2 Blast-Only Simulations

SwRI conducted blast-only sympathetic detonation modeling using CTH to estimate the response of both zinc- and steel-cased shaped charges to blast overpressures. Both charges had an N.E.W. of 23 grams of HMX-based explosive, but had significant differences in their geometry and case material. The digitized CT images were used to import the geometry into a regular 3D Eulerian mesh. Material models for the zinc, steel, donor Composition C-4 charge and receptor HMX were developed. A History Variable Reactive Burn (HVRB) model, previously validated during Phase I, was used for the energetic fill on both charges. A standard JWL was used for the Composition C-4. The donor charge position was varied until a Go/No-Go threshold was determined for both charges. A typical setup for the zinc charge is shown below in Figure 31.

[Not disclosed]

Figure 31. Zinc-Cased Charge (Left) and C-4 Donor (Right)

At a standoff distance of 0.50 inches, the 22-gram Composition C-4 charge, when detonated, did not have sufficient shock intensity to generate a sympathetic response in the zinc-cased donor charge. However, significant distortion of the receptor was indicated in the simulations. When the donor was moved into contact with the zinc-cased receptor (0-inch standoff), a high-order response was noted in the receptor.

<i>[Not disclosed]</i>	<i>[Not disclosed]</i>
Material Plot	
Pressure Plot	
Reaction Plot	
In-Contact (Go)	0.50-inch Air Gap (No-Go)

Figure 32. Zinc-Cased Charge Response to a 22-gram C-4 Donor

The same set of simulations was conducted for the heavier steel-cased shaped charge design. However, even when the bare donor charge was detonated in direct contact with the case, no high-order response was seen in the interior HMX-based explosive billet. Some deformation to the case was expected based on the results of the simulations.

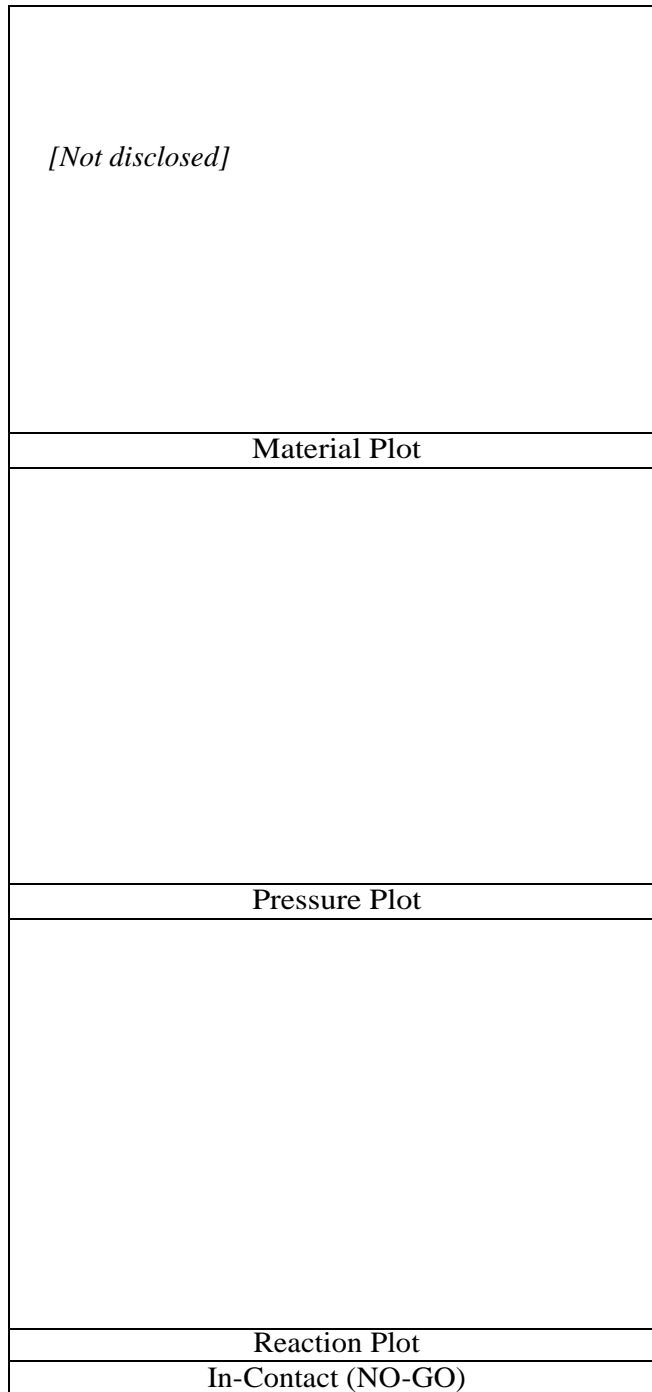


Figure 33. Steel-Cased Charge Response to a 22-gram C-4 Donor

The CTH results were in excellent agreement with the blast-only experiments detailed in Section 2. No-Go responses were noted in the zinc-cased charge at a 0.50-inch standoff, while sympathetic detonation was seen when the donor was detonated in-contact with the zinc. Even in the in-contact condition, the steel case was sufficient to prevent transmission of detonation into the receptor. The models proved useful to estimate the response of receptor and showed how the case affects the inherent sensitivity of the shaped charge design even at similar N.E.W.s and explosive fills.

3.3 Fragment Impact-Only Simulations

CTH was used to simulate the impact of an L/D=1 4340 steel cylinder into the side of both the steel-cased and zinc-cased shaped charges. The velocity of the fragment was varied in CTH until the Go/No-Go threshold was determined from both charges. The HVRB model was again employed for the energetic fill and the same steel model (strength, failure, and equation of state) used for the steel case was applied to the fragment. The results are shown below in the reaction plots in Figure 34.

[Not disclosed]

Steel Case with Steel Fragment Impactor

Zinc Case with Steel Fragment Impactor

[Not disclosed]

Figure 34. Fragment Impact-Only Sympathetic Detonation Simulations

The results of the CTH simulations did correctly identify that the steel-cased charge would be less sensitive to initiation than the zinc-case. However, the simulations over-predicted the velocity required to induce a detonation in the zinc charge (~4,400 fps in the simulation compared to less than 2,980 fps in the experiments). The simulation approach did show one advantage; the velocity of the fragment is not limited by the performance of the gun system. CTH can be used to simulate conditions difficult to achieve in cost-effective experiments. The inconsistency in the CTH results to the zinc-cased experiments warrants further investigation.

3.4 Combined Blast and Fragmentation Simulations

A single CTH simulation was conducted to mimic the combined blast and fragmentation sympathetic detonation experiments conducted during Phase II. A steel-cased donor charge was positioned 1 inch from a zinc-cased receptor charge. A JWLV with prescribed burn model was used in the donor charge while the HVRB model was used in the zinc receptor. The donor was detonated at top dead center and the resulting blast overpressure and fragment field was allowed to impact the neighboring donor. No high-order response was noted in the simulations. This is in excellent agreement with the experimental results and shows the insensitivity of the zinc-cased charge (1.4D).

<i>[Not disclosed]</i>	<i>[Not disclosed]</i>	<i>[Not disclosed]</i>
Material Plot	Pressure Plot	Reaction Plot
In-Contact (NO-GO)		

Figure 35. Combined Blast and Fragmentation (Steel Donor, Zinc Receptor)

3.5 Thermal Cook-off Modeling

FRC conducted an end-to-end calculation to show the workflow required to do a complete cook-off simulation and fragmentation of a charge in a simulated Series 6C (bonfire) test. The effort required multiple unique simulations to estimate the fragment field generated by the charge after cook-off. No analogous experiment was conducted to validate the results; rather, the simulation was for demonstration purposes and to exercise the approach.

First, thermal boundary conditions were applied to the steel-cased shaped charge with an HMX-based explosive fill. An implicit thermal-chemistry, reactive-flow cook-off simulation was performed with the

model to determine the thermal conditions and locations of a runaway reaction within the energetic fill. The severity of the response can also be determined (high-order, deflagration, etc.) based on the chemical material model and the reactions used to describe the chemical path between the initial energetic fill and the high-energy products. Variations in explosive type (PETN, HMX, HNS) can be explicitly studied. If a location of a runaway reaction was indicated in this analysis, a second simulation was run to determine the resulting case fragmentation and blast pressures.

<i>[Not disclosed]</i>	<i>[Not disclosed]</i>
Initial Mesh and Materials	Tracer Locations to Monitor Thermal Gradient
Temperature vs. Time at Various Locations	Temperature vs. Vertical Position
HMX Chemical Reaction Product Generation	Location of Runaway Initiation

Figure 36. Implicit Cook-off Model Results

The detonation point indicated in the implicit cook-off model was then used as input to a second simulation using traditional energetic models and techniques. In this case, a coupled Eulerian explosive was coupled to a SPH model of the steel case and copper liner. The explosive was detonated at the point indicated by the thermal analysis and the case was allowed to fracture and expand based on this off-axis initiation. The resulting fragments were monitored for velocity and energy (Figure 37).

<i>[Not disclosed]</i>	<i>[Not disclosed]</i>
SPH Case Expansion	Fragment Velocity and Energy

Figure 37. Subsequent Detonation Results with an SPH Case

4. METHODS FOR DETERMINING HAZARD CLASSIFICATION

SwRI and FRC have identified four (4) potential methodologies that can be used to classify shaped charges based on their inherent sensitivity to sympathetic initiation under normal shipping, storage, and handling conditions. They are listed below.

Method #1 – Continued Testing

Method #2 – Empirically-Based Metrics Derived from Historical Test Data

Method #3 – Analytical Techniques

Method #4 – High Fidelity Modeling and Simulation

Method #1 is currently being used by industry and has been formally documented in United Nations (UN) Manual of Tests and Criteria “ST-SG-AC10-11 Revision 5”. This allows for vendors around the world to utilize a common classification system whose tests can be replicated at various third party test labs and industry-owned sites. Additionally, it has the advantage of historical precedence, low cost due to extensive

industry experience, and the method of analysis has direct ties to realistic environments that a shaped charge could experience, such as rough handling during transport, an automotive crash, accidental fire, and unintentional detonation. Additionally, some vendors only rarely need to conduct Series 6 testing. As such, the current method of classification does not significantly influence their business model. Drawbacks include the cost and time associated with conducting the testing, cleanup hazards for the recovery of unreacted and unexploded charges, and the analysis required to report and interpret the results. The validity of the results can also be questioned due to the lower number of repeat tests required. Probabilistic variability of the results were not considered.

Method #2 would involve compilation of an extensive database of Class/Division assignments for previously designed and tested charges. Parameters, such as explosive type, case material, charge weight, case weight, package spacing, and test results (6A/B/C) would be compiled. SwRI and FRC provide an example of a set of metrics for default classification, based on empirical results, in the following section. Trends in the resulting Division assignments could then be used to generate empirical metrics.

The advantage of this technique for methodology development is that it would be widely backwards compatible by nature. Drawbacks of this method include protection of vendor's proprietary information, and inconsistency in the Series 6C test outcomes, and other than 1.4 Division assignments. SwRI reviewed a particular test report in which a small aluminum cap used to seal the top of a shaped charge would not release during bonfire testing; as a result, the charge would respond with a near high-order detonation (1.1 assignment). However, when the cap was replaced with a simple piece of foil tape, the exact same charge design obtained favorable results and a 1.4D hazard classification. Additionally, vendors often retest shaped charge designs, which previously failed a Series 6C test, with improvements to achieve the desired final Division assignment. As such, the empirical method would not include those "failed test results".

Methods #2 – 4 will be discussed in detail in the sections below. A background on Method #1 was described extensively in the Phase 1 Final Report.

4.1 Method #2 - Historical Shaped Charge Classification Data (Default)

When considering default classification metrics, such as N.E.W. or M/C ratios, a large volume of legacy classification data exists for charges, which are or were previously offered for shipment. Any proposed classification methodologies should be able to fit historical Class/Division assignments with a minimum number of outliers. SwRI conducted a detailed review of openly published data from numerous commercial shaped charge manufacturers to catalog and identify N.E.W. (C), case mass (M), explosive type, and M/C ratios for a wide range of both 1.1D and 1.4D shaped charges. The data set was then used to identify trends in previous Class/Division assignments by simplified metrics. The purpose of this exercise was to determine if any metrics could be identified from the dataset and to better understand the current delineations between 1.1D and 1.4D Division assignments.

Vendor specification sheets, product catalogs, on-line shipping information, and industry outreach through the Institute of Makers of Explosives (IME), were referenced to pull information on approximately 675 unique shaped charges from five (5) different U.S.-based vendors. Only one (1) vendor provided information through the industry outreach. In the majority of the cases, total explosive weight (C) and

explosive type was available. However, depending on the source, it was often difficult to determine case mass (M).

First, the data set was simply sorted by Class/Division assignment and N.E.W. The data was then binned into groups of 10-gram multiples (0 – 10 grams, 10 – 20 grams, etc.). Out of the total dataset (675), only 46 1.1D (UN 0059) items were identified. The vast majority of these were between 40 – 60 grams total N.E.W. The remaining charges all fell into a 1.4 Class/Division assignment. The most common N.E.W. being 20 – 30 grams followed by 10 – 20 grams and lastly, 30 – 40 grams. There was a slight overlap in the data sets around the 40-gram N.E.W. threshold (shown below in Figure 38). Thus, a simple N.E.W. metric of 40 grams could be proposed and would be consistent with the majority of the historical Class/Division assignments.

[Not disclosed]

Figure 38. Example Vendor Specification Sheet (from DynaEnergetics)

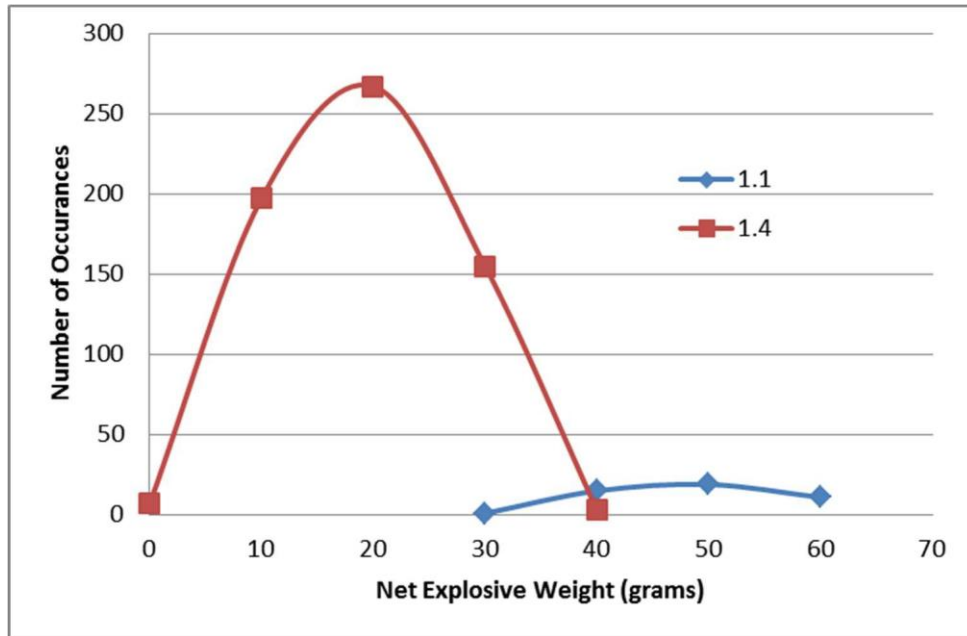


Figure 39. Class/Division Assignment as a Function of N.E.W.

The 40-gram threshold may be tied to the sand disruption requirement in the Series 6A/B-style testing where displacement of the sand confining material used in adjacent boxes surrounding the donor charge would result in a 1.1 Division assignment. In typical packing configurations, the pair charge orientation ensures that both the donor and the charge directly impacted by the donor jet will undergo high-order detonation resulting in twice the explosive yield during testing. This theory was tested during subsequent Phase 2 live-fire blast testing.

However, there was a zone of overlap which warranted further investigation. Only one (1) 1.1 Class/Division shaped charge was noted below a 40-gram N.E.W., and three (3) 1.4D assignments were noted above 40-grams. The particular 1.1D shaped charge had a particularly low M/C ration (3.0) indicating that there was a significant amount of explosive mass for the given case weight. The three 1.4D charges over 40-grams had an M/C ratio of approximately 6.5 which was much larger than normal for a 1.1 Class/Division shaped charge in the same N.E.W. range. Typical M/C ratios for the 1.1 Class/Division charges ranged from 3.00 – 5.25 while the 1.4 charges were much heavier in terms of case weights with M/C ratio ranging from 3.25 to almost 17. Thus, a simple combination of a N.E.W. threshold in combination with a minimum M/C ratio could be used to exactly bin the legacy charges without exception. An example is shown below in Table 8. A minimum M/C ratio of 3.5 could also be proposed for all 1.4 Class/Division charges and would be backwards compatible with a minimal number of outliers.

Table 8. Example Combined N.E.W., M/C Classification by Default Structure

N.E.W. (grams)	M/C (ratio)	Class/ Division
45 <	any	1.1
40-45	< 4.5	1.1
40-45	> 6.0	1.4
< 40	3.50	1.4

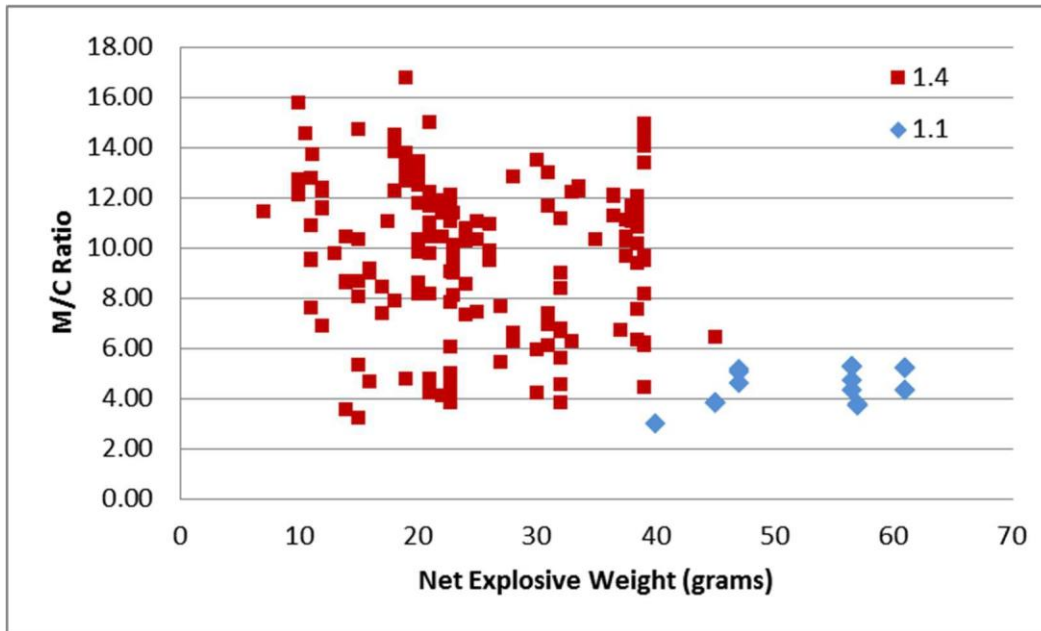


Figure 40. M/C Ratio as a Function of N.E.W. for both 1.1 and 1.4 Shaped Charges

The M/C has significant importance in the context of a Series 6A/B-style test in which neighboring charges within the donor’s package will be impacted by radial fragmentation generated by the donor charge. A higher M/C ratio typically results in slower, more massive radial fragments due to the thicker case mass. It also can result in improved resistance to shock initiation due to fragment and blast or combined fragmentation and blast. Lower M/C ratios can cause higher velocity radial fragments, which are more likely to elicit a sympathetic response in neighboring charges.

Unfortunately, SwRI and FRC were unable to fully compile information about the case material during the historical charge study. Some of the generalizations above may only be applicable within cases of a common material. As evident in the Phase 2 live-fire testing, the zinc cases tended to generate very fine light-weight fragments, which were almost dust-like when intentionally detonated. These present minimal hazards to neighboring charges. It is quite possible that further investigation could define combined N.E.W. and M/C metrics for steel and zinc cases. It should be noted that the zinc cases were also more prone to sympathetic detonation when tested against blast-only stimuli. Detailed information on charge spacing in the interior packaging was also not compiled and is important to overall susceptibility as seen in the Phase 2 testing.

Interestingly, there was no differentiation in the Class/Division assignment based on explosive type. This was slightly unexpected given the inherent shock sensitivity of the neat explosive formulations (PETN vs. RDX/HMX vs. HNS). It appears that the major reason vendors offer different explosive formulations is purely based on their resistance to down-hole temperature resistance. Formulations, such as NONA, PYX, and HNS, are more temperature resistant and can be left down-hole in loaded perforation guns for much longer durations prior to detonation. This gives oilfield workers more flexibility in their shot planning. However, high temperature rated explosives are prohibitively expensive in most applications.

[Not disclosed]

Figure 41. Down-Hole Time Rating vs. Temperature (from GEODynamics)

Upon further consideration, there are additional realities which can explain this finding. First, there are only two (2) Class/Division assignments into which oilfield perforation charge fall; 1.1D or 1.4D. As such, any charge design with an HMX/RDX-base found to have a 1.4D assignment cannot achieve a “lower” hazard rating by changing to HNS (a less sensitive explosive formulation). Many times companies only test the most sensitive charge designs, and accept the Class/Division assignment for all energetic formations in that standard design (case/liner). More delimitation may have been present if additional Class 1 Division assignments were possible. Additionally, highly sensitive formations, such as PETN, are not commonly used in oilfield shaped charges due to their poor performance at elevated temperature. Only one vendor surveyed during Phase 1 continues to use PETN in their typical product line. As such, this formulation was not present in the compiled dataset.

It should also be noted that the metrics proposed in Table 8, above, did not involve an understanding of which failed test resulted in the 1.1 Class/Division assignment. Future research efforts utilizing this approach should strive to incorporate this parameter during the initial database development. Variations in explosive density, packaging arrangement, and thermal environment during the bonfire test, could all generate different results during Series 6 testing.

4.2 Method #3 – Hazard Classification through Analytical Modeling

During the Phase 1 research, SwRI identified analytical methods for assessing the likelihood of sympathetic detonation of cased bombs, artillery shells, mortars, and warheads. The methodology has been used in the DoD community for safety studies and insensitive munitions efforts for the storage of cased ordnance in stack configurations. The orientation of the charges, methods of propagation of initiation, hazards, and parameters of interest are very similar to the smaller scale shaped charges used in the oil and gas industry and is directly applicable to a Series 6A/B-style test. The analytical techniques are well documented, founded in the physics of the problem, and can be leveraged without significant computational requirements.

Department of Defense Explosive Safety Board (DDESB) document “Simple Analytical Relationships for Munition Hazard Assessment” and “Sympathetic Detonation Predictive Methods” published in Wright Laboratory, Armament Directorate report WL-TR-93-7001 both contain detailed procedures about estimating the possibility of sympathetic detonation of neighboring charges. The technique considers the sensitivity of the explosive fill, critical diameter of the explosive, run-to-detonation distances for given shock pressures, case thickness and material (M), charge radius and spacing, and total explosive weight (C).

First, as in a Series 6A/B test, it is assumed that an interior charge in an array of vertically oriented charges, that a detonation occurs. The resulting velocity of the case fragments is determined using the Gurney equation. The Gurney equation is an analytical approach for estimating fragment velocities based on charge configuration (sandwich, cylinder, flat plate, etc.), charge mass (C) and case weight (M). A Gurney velocity (v) is required and is determined empirically or estimated based on the loaded density of the explosive. For conical shaped charges, the cross-section can be decomposed into multiple axial slices to calculate the velocities’ gradient across the height of the charge as the M/C ratio changes with cross-section.

Then, the effective size of the resulting case fragments can be estimated based on charge spacing, case material, char radius, and sound speed of the case material. Confinement (charge spacing that is insufficient to allow for charge expansion beyond 1.65 times the original charge radius) can generate larger fragments due to the interaction with neighboring charges. Shock physics equations are then used to estimate the pressures induced in the neighboring case wall and subsequently transmitted into the explosive. The transmitted pressure is then compared to Pop-plot data (run-to-detonation) information and the critical diameter of the explosive at the point of impact. This will determine if the pressure threshold for initiation is achieved and if the insult has sufficient distance (explosive thickness) to run up to a full detonation.

Advantages of this technique are its simplicity and historical precedence. The equations and relationships can be easily solved with simple programs or spreadsheet functions. However, the approach does require a comprehensive understanding of the Gurney velocity for a given explosive formulation and its inherent sensitivity to shock (Pop-plot). In many cases, due to the method of manufacturer, the exact density of the energetic is not known. Unfortunately, density plays an important role in the sensitivity of a given energetic. Also, the relationships for effective fragment size were developed for case materials such as steel (not zinc) and may need to be revised for less robust charges. Interior irregularities in the case wall, common in commercial shaped charges, can also change the shape and magnitude of the transmitted shock pulse to the explosive (Figure 42). Further investigation into this issue is outside the scope of the current effort.

[Not disclosed]

Figure 42. Example Case Geometry with Internal Serrations

During the course of this research, SwRI and FRC did not identify analogous analytical techniques for estimating the response of cased munitions to slow cook-off. This is a major drawback of Method #3 as bonfire testing (Series 6C) is required by current hazard classification specifications and represents a realistic environment during storage and transport.

4.3 Method #4 – Hazard Classification through Modeling & Simulation (M&S)

The last method considered by SwRI and FRC to determine Class/Division assignment was a complete end-to-end three dimensional simulation of response of shaped charges, in their packaging, subjected to Series 6 testing. This is not a default classification system, rather the response of the charges to simulated Series 6 test conditions would be explicitly modeled. The effort would involve capturing and importing the geometry of each unique charge design, their packaging, and the packing arrangement. This either requires explicit mesh development if traditional finite element techniques are employed or importation of volume domains (STL or similar) if Eulerian solvers are utilized. Then, material properties for equation of state, strength, and thermal response must be input for each of the components in the model (explosive, liner, case, dividers, exterior packaging, etc.). The external stimuli (intentional detonation for Series 6A/B or thermal load for Series 6C) must be applied as appropriate. Then the simulation must be executed and allowed to run to completion. For a Series 6A/B simulation for sympathetic detonation and disruption of confinement material, this may require the computation to run out to many milliseconds. For thermal models (Series 6C), the solution will require up to 30 minutes or more in the time domain.

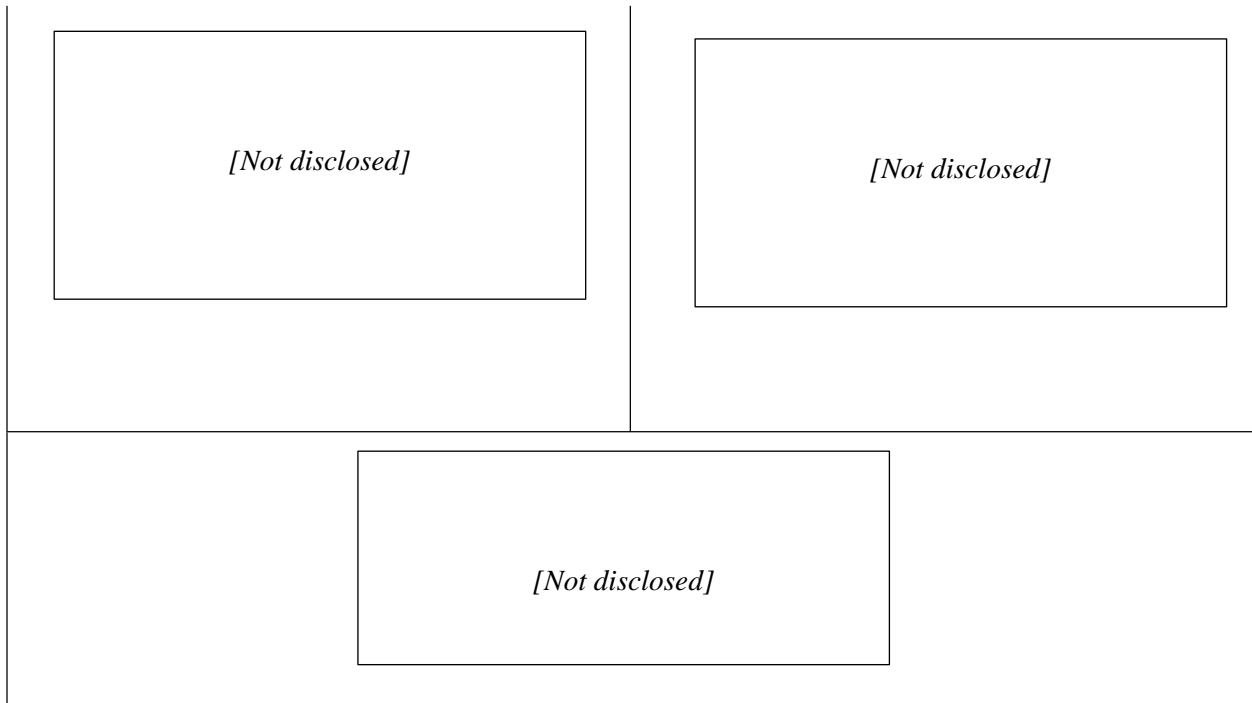


Figure 43. Finite Element Mesh for a Single Tray of Shaped Charges

To simulate a Series 6A/B test, a single charge would need to be intentionally detonated. That charge would likely utilize a JWL equation of state and a prescribed burn initiation method. The resulting explosive product expansion, shaped charge jet formation, and case expansion modeling process is relatively straightforward and well known to industry. A detailed strength and fracture model would be required to model the fragmentation of the case material. It is important to correctly model this process if radial fragmentation is the governing mode of sympathetic initiation. The neighboring charges would utilize a reactive explosive material model to assess the potential for sympathetic initiation. These material models (such as History Variable Reactive Burn and Ignition & Growth) are more sophisticated, but do exist for some explosive utilized in the defense industry. The commercial shaped charge industry would need to develop and validate similar models or select appropriate analogs based on the sensitivity of their proprietary explosive formulations. The modeling technique would then need to be validated against known experimental data to ensure accuracy of the results.

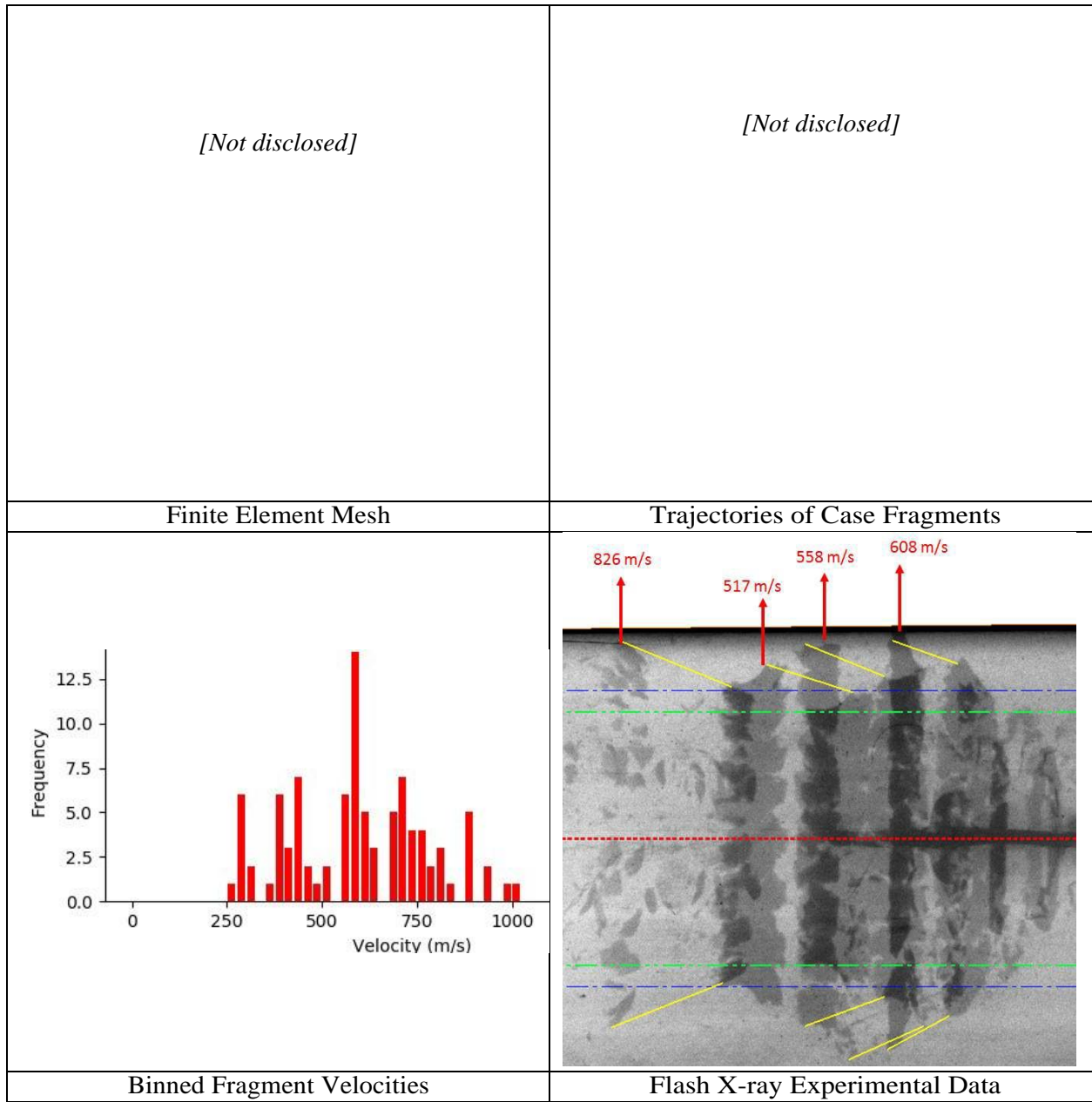


Figure 44. M&S of Intentionally Detonated Shaped Charge Case Fracture and Experimental Data

Simulation of a Series 6C event is more complicated than the previously discussed Series 6A/B intentional detonation testing. It requires specific information on the thermal loading generated by the wood crib or pool fire on the suspended packages. The breakdown of the packaging and internally arranged shaped charges then needs to be appropriately captured. The explosives undergo thermal decomposition, phase change, and may or may not respond with a severe runaway reaction. The result of the runaway reaction then needs to be calculated and the response of neighboring charges determined.

This process often involves a two-step modeling approach; thermal modeling followed by fragmentation modeling. A thermal analysis is conducted, which explicitly models the thermal loading imposed by the

bonfire and the thermos-chemical response of the energetic material. If a runaway reaction is indicated by the thermal analysis, a second simulation is conducted using the output from the thermal analysis as a detonation input to the fragmentation analysis (similar to that used for the Series 6A/B testing). Initiation and subsequent fracturing of the case is modeled and the fragment and blast over-pressure is allowed to interact with nearby charges.

<i>[Not disclosed]</i>	<i>[Not disclosed]</i>
Finite Element Mesh for Thermal Analysis	Thermal Gradient due to Uneven Heating
<i>[Not disclosed]</i>	<i>[Not disclosed]</i>
Location of Runaway Reaction	Location of Initiation of Explosive Billet

Figure 45. FRC’s Simulations of Thermal Initiation of a Shaped Charge

The modeling requirements for simulating Series 6A/B testing are fairly mature and could be easily replicated by qualified engineers in the commercial shaped charge industry. However, the bonfire event (Series 6C) is a very complicated thermal environment. Knowledge about the sensitivity of energetics at elevated temperatures is required. Detailed material models must be used to describe thermal heating and decomposition of the energetics and the severity of the response must be accurately captured. Breakdown of the exterior and interior packing means that the exact positioning of the charges within a given package changes throughout the event. These factors present significant barriers to entry for organizations wishing to conduct detailed simulations of the Series 6C testing. Further research in this area has been proposed later in this report.

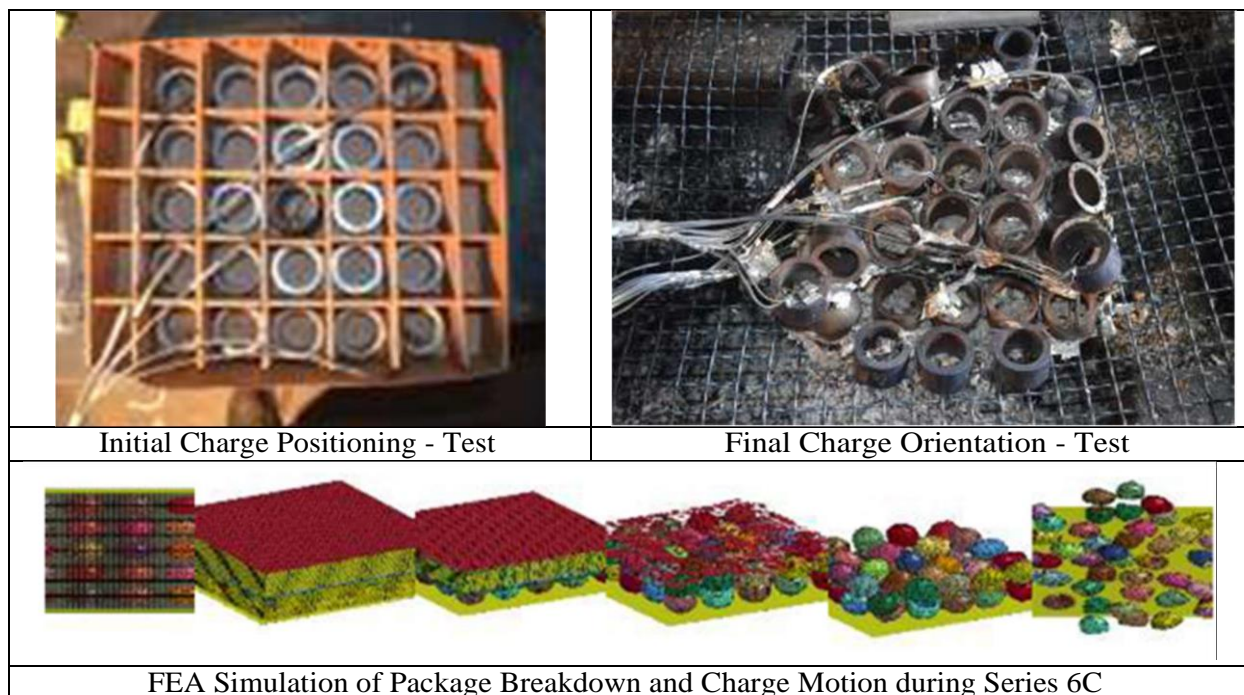


Figure 46. Charge Position in a Simulated Bonfire Test

The main advantage of a combined M&S approach is the potential for the probability of response to be estimated using a Monte Carlo-style analysis in conjunction with the M&S. The various parameters of interest (geometry, material properties, material response, positioning, thermal environment, etc.) all vary from lot to lot and test to test. A probability function can be assigned to these variables and numerous iterations can be run to determine the likelihood of a particular response to a given test. Various charges in a package could be detonated to study the response of an exterior, interior, or edge charge detonation in a Series 6A/B test. The package material and spacing could be varied to determine thresholds for particular charges without the need to run a complete bonfire test. This type of analysis would be cost effective once an accurate model is developed and could potentially identify the parameters which most strongly influence the response of a given charge and packaging configuration.

A major drawback of the M&S method for classification is the requirement for highly detailed reactive explosive models for both shock initiation and thermal runaway reactions. The majority of the models used by both SwRI and FRC during this activity were previously developed by the Department of Defense and the Department of Energy for defense applications. The models are for industry-accepted formulations rather than for proprietary formulations and processes. The testing required to develop run-to-detonation data and thermal reactivity requires specialized equipment and costly experimentation. Industry shaped charge manufacturers would be required to fully characterize each of their unique energetic formulations and develop these models prior to executing an M&S effort. This may be prohibitive from an industry acceptance perspective.

Computational hardware requirements are also significant. Multi-processor systems are required to run the 3D simulations. The long time durations required for the thermal cook-off modeling also increase computational requirements. Some of the software distribution is regulated by the DoE and others have

annual license requirements. Shaped charge vendors would need to acquire sufficient infrastructure to support the computations. All these considerations must be taken into account when determining the likelihood of industry acceptance.

Acceptance of the results of an M&S analysis by regulatory agencies must also be considered. The complexity of analysis, material model development, and comparison to validation data would require a high level of understanding by personnel in the regulatory agencies reviewing the results. This could present some institutional resistance to moving away from physical testing and into a more virtual analysis of the hazards. It is also difficult to disagree with well conducted experimental results for shaped charge sensitivity. The results are more tangible and defined (Pass/Fail) making them more palatable from a risk perspective.

5. CONCLUSIONS ON METHODOLOGIES

During both the Phase I and Phase II research efforts, SwRI and FRC investigated the parameters associated with sympathetic initiation of shaped charges due to intentional detonation or bonfire testing as specified by United Nations (UN) Manual of Tests and Criteria “ST-SG-AC10-11 Revision 5”. Industry partners and various stakeholders were identified and engaged during the Phase I effort to better understand the testing, general EX application process, oilfield shaped charge manufacturing and uses, design parameters, and other drivers of their hazard classification. Then, during Phase I and Phase II, SwRI and FEC both conducted instrumented live-fire experiments and high-fidelity modeling of shaped charges under various forms of external insult. Additional studies also focused on compiling information about shaped charges that had previously been assigned a hazard classification to see if any delineation were notable in the historical data.

Based on the work conducted during this project, FRC and SwRI have been able to demonstrate and conclude the following:

- The fragmentation characteristic of an initiated shaped charge are primarily driven by the energetic formulation and cases material and geometry. Equivalent case designs can produce varying distributions of fragment sizes, counts, and velocities when used with differing explosive types.
- Case fragmentation characteristics are sensitive to location of initiation (i.e. center vs. offset detonation).
- Packaging material and the resulting shaped charge separation can prevent sympathetic detonation.
- Sympathetic detonation due to fragment impact and jet impingement can be readily replicated. The threshold for detonation response is highly dependent on the explosive formulation. A lack of validated ignition and growth models precludes the ability to thoroughly and accurately investigate the effects of explosive formulations used in industry due to lack of information regarding billet density.

- The heat flux resulting from a bonfire test is highly dependent on the fuel source, the ambient conditions, and the geometry of the test setup. These results have been confirmed through both numerical and physical testing. Liquid fuel produces a more controllable and steady heat release rate.
- Detonation in a bonfire test is related to the explosive formulation and containment provided by the case/liner. Energetic materials of interest to this project are able to detonate under the thermal conditions provided by a bonfire. However, the lack of pressure build-up within the case/liner precludes a high-order response and generally results in low-order deflagration only.
- Shaped charge temperature varies across the package and across the exterior of a given shaped charge during a bonfire test. Differences of 10 – 50°C are observed across a single shaped charge and differences of up to 200°C are observed between various shaped charges across the package.
- Case geometry and material selection directly affects the thermal response of the explosive fill. Localized heating due to geometrical variations can result in asymmetrical heating.
- Asymmetric heating results in deflagration or detonation being initiated in an offset manner (generally near the connection between the liner and the case). As mentioned above, this asymmetric initiation directly affects the resulting fragmentation characteristics.
- The effect of packaging design on shaped charge performance in a bonfire test needs further research. For materials easily consumed in a bonfire test, such as fiberboard, the package often disintegrated prior to the shaped charges being affected resulting in a jumble of shaped charges directly exposed to the fire.

The purpose of the Phase I and Phase II efforts was to better understand the parameters affecting the resulting Class/Division assignment of shaped charges based on their inherent sensitivity. Then, using this knowledge, draft metrics for default classification could be developed and proposed. Default classification criteria would allow for new charge designs to be hazard classified without the need for additional testing. In Section 4 of this report, SwRI presented an example of what a set of metrics might look like and discussed other methodologies for classification without Series 6 testing.

The table below provides a notional comparison between the four methodologies described in Section 4. Six (6) unique metrics were rated on a scale of 0 – 10, with 10 being the highest possible rating (good) and 0 as the lowest (bad). They were color coded for display purposes in a hot-cold format (ROYGB), low to high. The values for each rating were developed by SwRI and FRC based on the lessons learned during both the Phase 1 and Phase 2 activities. The chart below shows that there is obvious historical precedence and industry inertia to continue to use the current method for classification (Series 6 testing). It is cost effective, already accepted by industry and regulatory bodies, and provides reasonable classifications. (SwRI and FRC were unable to identify any incidents involving the energetic response of shaped charges during transport/storage during Phase 1.) Many of these same advantages are also realized by Method #2 (Historical Metrics for Default Classification). Additionally, by including a significant number of test results in the dataset, some level of probability is built into the system.

Table 9. Visual Comparison of Methods to Develop Default Classification System

	Methodology			
	1	2	3	4
Ease of Use (Complexity)	8	10	6	4
Cost to Conduct	8	10	8	6
Probabilistic Component	0	4	10	10
Historical Precedence	10	10	6	6
Accuracy	10	8	2	4
Likelihood of Acceptance	10	8	4	4

Both the analytical modeling (Method #3) and the high fidelity modeling and simulation approach (Method #4) suffer from technical complexity and low likelihood of industry acceptance. Detailed material response models for the explosives and case materials are required for the M&S approach. Often, this requires costly experimentation to determine the model parameters and the computations must be run on high performance computers. Additionally, there is little historical precedence for an approach requiring no actual hazard testing and, thus, the acceptance by shareholders is unlikely. However, significant probability of outcome can be built into this type of analysis via a parametric analysis. Material properties, geometry, thermal environment, and other parameters can be varied of subsequent iterations to determine the complete response spectra. Once a model is developed, automation and scripting can be leveraged to expedite the analysis. These techniques would also let charge designers identify which components of the charge have the biggest effect on the resulting hazard classification.

Based on Table 9, SwRI and FRC recommend that the draft metrics presented in Section 4.1 be further developed by the inclusion of additional charges and validated with larger scale testing and M&S efforts. Section 6 discusses the recommended research to fully vet these metrics.

6. RECOMMENDATIONS AND FURTHER RESEARCH

SwRI and FRC recommend that the draft metrics for default classification be modified based on the results of a more comprehensive historical database development for oilfield perforation shaped charges. The following recommendations are made for the expansion on the existing data set.

- 1) Increase the total number of charges in the database, especially those with a 1.1D Class/Division assignment. Where possible, include historical charges which are no longer sold or offered for shipment.
- 2) Differentiate between zinc- and steel-cased charges.
- 3) Include the actual case mass (M) in the M/C ratio. (Not the combined case and liner mass.)
- 4) Compile spacing (row and column) information.

Expansion of the current shaped charge database will provide more comprehensive metrics to be developed based on historical EX application testing. This will provide more delineation at the boundaries between 1.1D and 1.4D Class/Division assignments. Industry outreach through professional organizations, such as the Institute of Makers of Explosives, particularly the Oilfield Services Subcommittee and PHMSA Subcommittee, should be undertaken to improve manufacturer participation and gain access to the recommended additional information below. PHMSA, themselves, should also promote this effort at their annual meeting with the Explosive Examiners.

As seen in the Phase II testing, zinc cases differ significantly from steel in the fragment field they generate and in the shock buffering they provide during impact. While explosive formulation is compiled, the current shaped charge database does not differentiate with respect to case material in the reported M/C ratio. With a sufficient number of charges included in the database, SwRI and FRC can more definitively state if there are notable differences in their resulting classification based on N.E.W. and M/C. It is possible that different metrics can be employed depending on the case material utilized.

In the current database, the case mass was determined from total unit weight information minus the explosive load. This means that both the actual case mass and the shaped charge liner mass are included in the calculation. The reason for this is that the mass breakdown for inert components for shaped charges is often not included in the product specification information. For heavy steel-walled cases, this is probably a reasonable approximation. However, for thinner cases or zinc-cased charges, this can become problematic. By including the actual case mass, rather than a combined case/liner mass, a more appropriate M/C ratio can be determined for assessing sensitivity to sympathetic detonation.

SwRI demonstrated, both computationally and experimentally, that charge spacing plays an important role in the potential for sympathetic detonation in the context of a Series 6A/B-style test. The metrics proposed in Section 6 of this report do not include charge spacing. This was omitted due to the limited availability of this information in open sources. Future improvements to the draft metrics should include minimum charge spacing and would likely involve simplifying the row/column spacing into a single parameter. Figure 47, below, shows the variation in charge spacing for the charges used in the Phase I and II testing.

<i>[Not disclosed]</i>	<i>[Not disclosed]</i>
<i>[Not disclosed]</i>	<i>[Not disclosed]</i>

Figure 47. Example Package Arrangements for Commercial Shaped Charges

Both SwRI and FRC feel that modeling and simulation provides an excellent complement to the experimental data. As such, a mirrored approach of combined empirical metrics and supporting M&S is proposed, similar to the work conducted in both Phases I and II of this effort. The following areas of research would enhance SwRI and FRC’s understanding of the problem set and allow for more accurate modeling.

Calibrate numerical models with a range of responses from low-order deflagration to high-order detonation for representative explosives. These responses can then be used to drive small- and large-scale models that investigate the full range of scenarios expected in both the UN test series (e.g. stack and bonfire tests) and real world scenarios (e.g. large payload heavy truck fire). The models could be calibrated to existing or new experimental data by scaling existing HE material models.

Identify the existing shaped charge designs that fail the bonfire tests. This will involve a combination of real world data and performance, coupled with finite element analysis to verify the hypotheses. Evaluate the failed design compared to those that pass the bonfire test. It is anticipated that those that fail are designed in a way that allows pressure to build up within the billet and/or have an explosive formulation that is more sensitive to heating or has impurities.

Conduct physical and/or simulated bonfire tests of shaped charges or surrogate shaped charges with varying levels of pressurization capability. Shaped charge designs that are capable of generating high pressures within the case/liner are more likely to experience a high-order response. Use existing data or generate new data as necessary for the explosives of interest from ODTX experiments. Characterizing the transient response of explosive from deflagration to detonation based

on temperature and pressure and validating numerical models with the results using chemistry, cheetah, and equation of state models for the explosive will provide better correlation with test results.

Investigate the sensitivity of sympathetic detonation due to fragment impact using controlled test methods on various shaped charge designs. The shaped charges will be impacted with fragments at select energy levels (mass and velocity of fragment) to determine thresholds for sympathetic detonation. The case geometry and material and explosive sensitivity are likely to be the main factors in determining the likelihood of sympathetic detonation.

Investigate the effect of temperature on sympathetic detonation due to fragment impact using controlled methods. It is known that increased temperature generally increases the sensitivity of explosive to shock-induced detonation. Further, as degradation of the energetic increases due to thermal exposure, the sensitivity of explosive could increase further. This work will investigate if increased temperatures representative of those reached in a bonfire test result in a greater likelihood of sympathetic detonation due to fragment impact. Validate numerical models with the results using ignition and growth material definitions for HE that are tuned to experimental data based on temperature response.

Investigate the sensitivity of sympathetic detonation due to overpressure (with and without temperature effects). Validate numerical models with the results using ignition and growth material definitions for the explosives of interest. Tune parameters to mimic results as necessary.

Investigate the thermal response of a deflagrating shaped charge. Characterize this response according to shaped charge design and explosive fill. A deflagrating shaped charge will generate high pressures (up to 1 GPa) and burn at high temperatures often greater than 1000 K. Material degradation of the energetic will occur due to extended heating scenarios, such as those produced in a bonfire tests. The deflagration of degraded HMX (LX-04 formulation) typically results in higher deflagration rates compared to non-degraded samples.

Measure effect of impingement of deflagrating shaped charge flame on neighboring shaped charge. Due to the likelihood of high-rate deflagration, it is highly likely that a deflagrating charge will apply a greater heat flux to a neighboring charge than the surrounding fire would apply to a neighboring charge if the thermal output, due to the deflagration of a single or multiple shaped charges, exceeds the critical shock energy. It is also important to investigate the effect of total shaped charge quantity in a given bonfire test. Does an increase in material increase the probability of mass detonation due to compounding heating and reactions?

Characterize the effects of various industry-utilized energetic formulations (type, binder type and % volume) on shaped charge fragmentation. Using cheetah, define the boundaries of theoretical burn models based on specific formulation inputs. Then evaluate the effect of these variations on fragment characteristics of the case. This effort can be conducted as parametrical sensitivity study fully within the numerical regime using ALE3D.